Self-assembly of temperature-responsive protein–polymer bioconjugates

Bioconjugate Chemistry

Article

pubs.acs.org/bc

Self-Assembly of Temperature-Responsive Protein−Polymer Bioconjugates

Dafni Moatsou,[†,#] Jian Li,[‡,#] Arnaz Ranji,[‡] Anaïs Pitto-Barry,[†] Ioanna Ntai,[‡] Michael C. Jewett,*[,‡] and Rachel K. O'Reilly*[,†]

[†]Department of Chemistry, University of Warwick, Gibbet Hill Road, Coventry CV4 7AL, United Kingdom

[‡]Department of Chemical and Biological Engineering, Chemistry of Life Processes Institute, Northwestern University, Evanston, Illinois 60208, United States

Supporting Information

ABSTRACT: We report a simple temperature-responsive bioconjugate system comprising superfolder green fluorescent protein (sfGFP) decorated with poly[(oligo ethylene glycol) methyl ether methacrylate] (PEGMA) polymers. We used amber suppression to site-specifically incorporate the non-canonical azide-functional amino acid *p*-azidophenylalanine (*p*AzF) into sfGFP at different positions. The azide moiety on modified sfGFP was then coupled using copper-catalyzed "click" chemistry with the alkyne terminus of a PEGMA synthesized by reversible addition−fragmentation chain transfer (RAFT) polymerization. The protein in the resulting bioconjugate was found to remain functionally active (i.e., fluorescent) after conjugation. Turbidity measurements revealed that the point of attachment of the polymer onto the protein scaffold has an impact on the thermoresponsive behavior of the resultant bioconjugate. Furthermore, small-angle X-ray scattering analysis showed the wrapping of the polymer around the protein in a temperature-dependent fashion. Our work demonstrates that standard genetic manipulation combined with an expanded genetic code provides an easy way to construct functional hybrid biomaterials where the location of the conjugation site on the protein plays an important role in determining material properties. We anticipate that our approach could be generalized for the synthesis of complex functional materials with precisely defined domain orientation, connectivity, and composition.

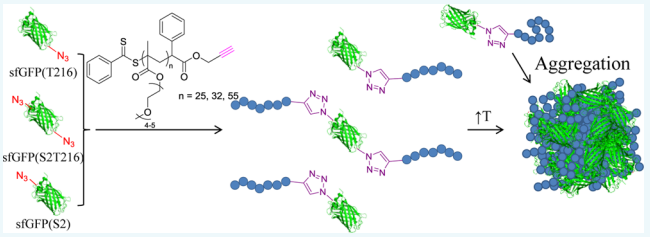

INTRODUCTION

Ever since the pioneering work of Davis and co-workers,[1,2] the conjugation of synthetic macromolecules with proteins to enhance the chemical properties and functions of the latter has been demonstrated for a variety of systems and a range of applications. Some illustrative examples include increased protein activity, proteolytic resistance, and thermal and pH stability,[3,4] properties that have been attributed to the careful selection of the molecular characteristics of the polymer and the conjugation site.[3] The vast majority of reports involve proteins conjugated with poly(ethylene glycol) (PEG),[5−8] as it is a biocompatible polymer with a proven record of applications.[3,4,8−11] Noteworthy also is the use of branched PEG analogues that have been shown to further enhance the biocompatibility of their protein bioconjugates.[12] Nevertheless, the use of polymers that endow the protein with more intricate properties has been sought, such as polymers that respond to external stimuli.[13,14]

Stimuli-responsive polymers can be used to expand the properties of protein−polymer systems,[15−17] owing to their ability to change their physicochemical properties as a response to small changes in their environment (i.e., temperature, pH, light, etc.) and their corresponding bioconjugates inherit that ability, obtaining a triggered (and commonly reversible) amphiphilic character.[18−24] Hoffman and co-workers pioneered the use of stimuli-responsive polymers for conjugation with proteins that allowed their isolation and reuse, or modulation of their activity.[25−29] In other examples, permanently amphiphilic bioconjugates,[18,19,30−32] whereby the protein is conjugated with a hydrophobic polymer, have shown potential in improving the protein activity (such as inhibition of tumor cell growth),[33] although in some cases the opposite effect was observed.[34,35] Similarly, stimuli-responsive bioconjugates (frequently referred to as "smart" bioconjugates[21]) are often studied as potential "on/off" systems,[36−38] whereby the solvation of the polymer dictates the protein activity.[39] In addition to the effect on protein activity, bioconjugates with an amphiphilic character (often referred to as "giant amphiphiles") form elaborate nanostructures as a result of their self-assembly in water.[30,32,34,40,41]

In building protein−polymer macromolecules, several design decisions must be considered. First, the strategy to attach the polymer to the protein must be defined. The most used conjugation method involves the functionalization of all available natural amino acid target moieties on the protein,[42−45] commonly lysine or cysteine residues. Other approaches have

Received: May 8, 2015
Revised: June 12, 2015
Published: June 17, 2015

DOI: 10.1021/acs.bioconjchem.5b00264
Bioconjugate Chem. 2015, 26, 1890−1899

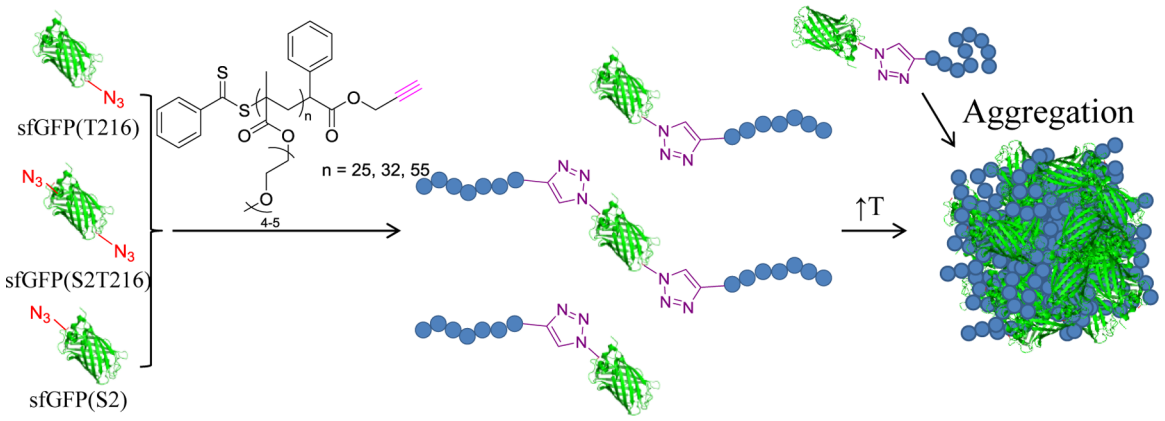

Figure 1. Strategy followed for the synthesis of sfGFP-PEGMA bioconjugates *via* the engineering of three sfGFP analogues with T216, S2T216, and S2 site modification with *p*AzF before the CuAAc of alkyne-functional PEGMA (three different molecular weights). Upon an increase of the solution temperature, all bioconjugates were found to aggregate.

targeted the *N*-terminus of the protein,[46,47] while in other examples a single available functional amino acid is targeted.[32,48−51] These synthetic approaches to decorating proteins have been extensively presented in numerous noteworthy reviews.[6,7,52−63] A recurring limitation in a large number of the reports in the literature is that covalent coupling leads to a heterogeneous mixture of products with varying conjugation degrees. This has been found to be related to the polymer molecular weight,[64] polymer docking location onto the protein, and also heterogeneities in the protein which affect the availability of the modification sites,[65] thus highlighting the need for complete control over the conjugation site.[20]

Recent studies have shown that the introduction of noncanonical amino acids (ncAAs) into a functional protein expands the available chemistries for conjugation,[66] allowing a higher degree of precision and minimization of side-reactions and byproducts.[67] In one approach, pioneered by Tirrell and colleagues,[68−72] all natural amino acids (typically methionine, isoleucine, or leucine) are globally replaced by a ncAA. While powerful, changing all occurrences of a natural amino acid in a protein may unfavorably affect protein folding and activity. In addition, the chemical diversity introduced *via* ncAAs in this procedure is limited since the ncAA must be a close analogue of the natural amino acid it replaces. In an alternative approach, ncAAs are quantitatively installed at defined sites in a protein through genetic code expansion. The most widely used strategy for expanding the genetic code is based on the amber suppression technique using orthogonal aminoacyl-tRNA synthetase/tRNA pairs.[73] Many seminal works from Schultz and others have established and driven the field forward, and more than 150 different ncAAs have been site-specifically incorporated into proteins to date.[66,74−76] These ncAAs normally carry functional moieties (e.g., aryl-azide) that do not exist in the canonical 20 amino acids and that are easy to chemically modify (e.g., using copper-catalyzed alkyne−azide cycloaddition[77−81]), although the success of the modification also relies on the conjugation site.[82] A notable example is the incorporation of a polymerization-initiating ncAA into green fluorescent protein (GFP) and the subsequent growth of a polymer from the surface of the protein.[83] Such modifications can thus allow conjugation with polymers which, as previously mentioned, could protect the protein from degradation or prevent the polymer interfering with the protein activity. Another significant advantage of this approach is that it can allow the introduction of ncAAs without altering the net charge or the redox potential of the protein, as is often the result of functionalizing lysine and cysteine residues, respectively.

After deciding how to precisely link proteins to polymers, the second key design consideration is polymer conjugation strategy. In one approach, the presynthesized polymer can be "grafted to" the protein. The major drawback of this approach stems from the difficulty removing the high-molecular-weight byproducts (i.e., excess polymer). An alternative strategy is to "graft from", where the protein is functionalized with a moiety that participates in the polymer synthesis, such as a polymerization initiator/mediator. Recently, such "grafting from" approaches have become more accessible since the development of reversible deactivation radical polymerizations,[57,58] such as atom transfer radical polymerization (ATRP), reversible addition−fragmentation chain transfer (RAFT) polymerization, and nitroxide-mediated polymerization (NMP) which allow the reaction to occur under conditions suitable for retention of the protein stability.[84] However, "grafting to" is still a popular conjugation method as it allows the fine-tuning of the molecular characteristics of the polymer before its conjugation.

Recently, several reports have begun to make possible new types of protein−polymer bioconjugates using GFP as a model protein.[85] Nolte and co-workers, for example, studied the self-assembly of conjugated biohybrid copolymers comprising GFP and poly[(oligo ethylene glycol) methyl ether acrylate] (PEGMA) and showed that the resulting biohybrid amphiphiles were thermoresponsive.[86] However, their study was limited to the use of natural amino acid handles for conjugation (i.e., cysteine) and was insufficient to study the impact of multiple polymers attached to the compact protein core. Similarly, Olsen et al. reported the conjugation of thermoresponsive polymers with a GFP via thiol−maleimide ligation. The resulting bioconjugates formed micelles when the solution temperature was increased.[87] In another example, Matyjaszewski and co-workers reported the incorporation of *p*AzF into a GFP and its subsequent bioconjugation with a PEG containing two alkyne functionalities. This resulted in a "step-growth" formation of micron-sized fibers that were attributed to the dimerization of GFP.[88] This was a significant advance in the study of properties of polymer−protein bioconjugates and it demonstrates the infinite potential applications that will emerge once more intricate polymers are explored in such systems. However, our understanding of how the location on the protein

DOI: 10.1021/acs.bioconjchem.5b00264
Bioconjugate Chem. 2015, 26, 1890−1899

surface of conjugation can affect the resultant properties of the protein−polymer bioconjugate material remains incomplete.

Here, we sought to build on these recent reports to demonstrate a simple bioconjugate protein−polymer system that would allow us to study the impact of site-specific conjugation on self-assembly and responsiveness. Our goal was to produce and study biomacromolecules comprising superfolder GFP (sfGFP) decorated with temperature-responsive poly[(oligo ethylene glycol) methyl ether methacrylate] (PEGMA) chains of different molecular weights on more than one site, by copper-catalyzed azide−alkyne cycloaddition reaction (CuAAc). Similarly to PEG, PEGMA has been shown to be biocompatible[33] and, additionally, exhibits a lower critical solution temperature (LCST) in water.[89] Our study involved three steps. First, the sfGFP molecules were functionalized with azide groups (at amino acid residues 2, 216, or 2 and 216). Second, the reactive azide moieties were conjugated with an alkyne-containing PEGMA synthesized by RAFT polymerization. Third, we characterized the reversible transition of the protein−polymer structures from a water-soluble to a water-insoluble state upon heating above a critical temperature (namely the cloud point). Our results showed that the resultant structures had properties of both the fluorescent sfGFP and the temperature-responsive PEGMA (Figure 1). Additionally, we explored the effect of different attachment positions on the protein on the cloud point of the bioconjugate using turbidimetry, dynamic light scattering (DLS), and small-angle X-ray scattering (SAXS) analysis.

RESULTS AND DISCUSSION

We began our study by producing the *p*-azidophenylalanine (*p*AzF) sfGFP labeled reagents. To incorporate *p*AzF into sfGFP, *Escherichia coli* BL21(DE3) cells were first co-transformed with the pEVOL-pAzF plasmid that encodes the aminoacyl-tRNA synthetase/suppressor tRNA pair[90] and an appropriate mutant pY71-sfGFP plasmid with amber codon (TAG) at positions of S2, T216, or S2/T216. These locations were chosen as the S2 and T216 residues are located at opposite ends of the protein's barrel structure on flexible loops that do not affect sfGFP folding. In addition, this design allowed us to introduce two conjugation points on opposite sides of the protein structure (Figure 1; see Figure S1 in the Supporting Information (SI) for more information on the sites of modification).

Then, the desired sfGFP proteins were overexpressed and purified from the BL21 (DE3) cells, noting that T7 RNA polymerase, which drives sfGFP transcription in pY71-sfGFP, was expressed from a DE3 λ prophage under an isopropyl β-D-1-thiogalactopyranoside (IPTG)-inducible *lacI* promoter in BL21(DE3) (see SI for methods). Protein expression yields were estimated to be ~20 mg/L by comparison of purified protein to standards of bovine serum albumin at known concentrations. With the purified sfGFP variants in hand, we carried out top-down mass spectrometry (i.e., MS analysis of whole intact proteins) to detect and provide semiquantitative information for the incorporation of *p*AzF into sfGFP. Figure 2 shows the 32+ charge state of sfGFP and clearly illustrates mass shifts corresponding to the incorporation of each of the specifically incorporated *p*AzF residues. Site-specific incorporation of *p*AzF, as detected by MS, was greater than 95% in all samples (Figure 2), noting that the experimental and theoretical protein masses were in good agreement (see SI, Table S2). In summary, we achieved efficient, high yielding, and

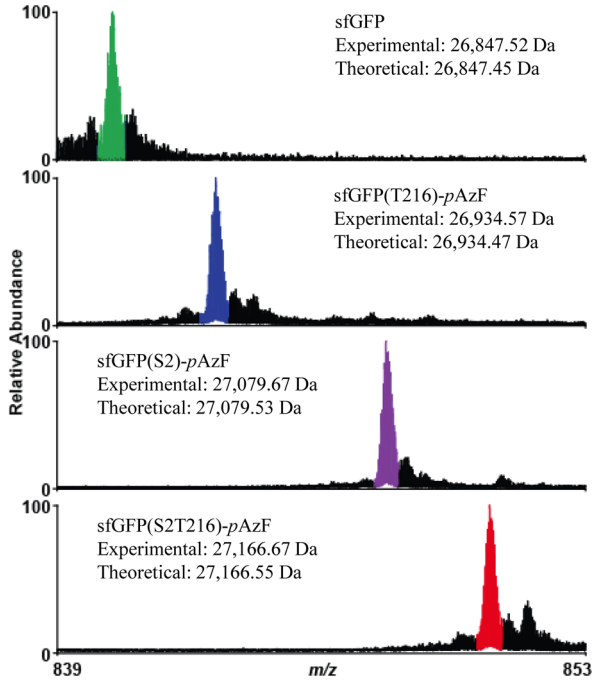

Figure 2. Mass spectrum of the 32+ charge state of sfGFP obtained via top-down mass spectrometry illustrating site-specific incorporation of pAzF at single and multiple sites. Major peaks in each spectrum coincide with the theoretical peaks for each species and have been highlighted. Smaller peaks to the right of the colored peaks are due to oxidation of the protein—a common electrochemical reaction occurring during electrospray ionization.[91] Water loss events from the intact sfGFP are detected at minor levels to the left of the major (colored) peaks. Note that the start (N-terminal) methionine of sfGFP is usually cleaved post-translationally by methionine aminopeptidase present in the *E. coli* proteome. However, the presence of an unnatural amino acid at S2 appears to hinder this enzyme (For more detail, see SI Table S2).

pure site-specific *p*AzF incorporation into sfGFP at two different sites at opposite ends of the protein barrel structure.

Once the production of pure modified proteins by mass spectrometry was confirmed, the accessibility of the reactive azide moieties was established by exploration of a CuAAC reaction with an alkyne-containing rhodamine B fluorescent dye (**1**) (see SI). All protein−dye bioconjugates were found to contain the rhodamine B dye by PAGE analysis (see SI, Figure S3), although LC-MS suggested incomplete conjugation (see SI, Figure S4). This highlighted that the two modified positions on the sfGFP were accessible for reaction using CuAAC.

For the conjugation of the protein with a polymer, an alkyne-containing chain transfer agent (CTA, **2**) was chosen for the RAFT polymerization of $OEGMA_{300}$ (Figure 1). Three polymers varying in molecular weight (Table 1) were synthesized by changes in monomer feed and reaction time

Table 1. Number Average Molecular Weights and Molecular Weight Distributions of the Polymers Used for the Synthesis of the Bioconjugates

polymer	M_n[a] (g/mol)	$Đ_M$
PEGMA-1	7600	1.26
PEGMA-2	9600	1.32
PEGMA-3	16700	1.36

[a]Determined by SEC in THF (2% triethylamine).

DOI: 10.1021/acs.bioconjchem.5b00264
Bioconjugate Chem. 2015, 26, 1890−1899

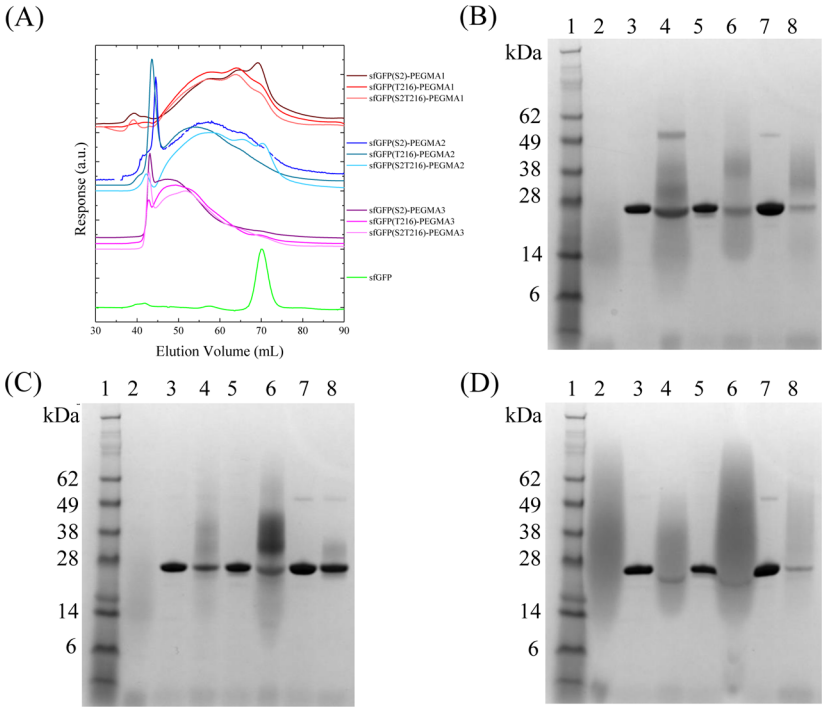

Figure 3. Comparison of the synthesized bioconjugates with their corresponding unfunctionalized protein and polymer: (A) Chromatograms from the crude protein−polymer bioconjugates, and (B) PAGE gels of the proteins upon conjugation with PEGMA-1: lane 1, ladder; lane 2, PEGMA-1; lane 3, sfGFP(S2); lane 4, sfGFP(S2)-PEGMA1; lane 5, sfGFP(T216); lane 6, sfGFP(T216)-PEGMA1; lane 7, sfGFP(S2T216); lane 8, sfGFP(S2T216)-PEGMA1; (C) upon conjugation with PEGMA-2: lane 1, ladder; lane 2, PEGMA-2; lane 3, sfGFP(S2); lane 4, sfGFP(S2)-PEGMA2; lane 5, sfGFP(T216); lane 6, sfGFP(T216)-PEGMA2; lane 7, sfGFP(S2T216); lane 8, sfGFP(S2T216)-PEGMA2; (D) and upon conjugation with PEGMA-3: lane 1, ladder; lane 2, PEGMA-3; lane 3, sfGFP(S2); lane 4, sfGFP(S2)-PEGMA3; lane 5, sfGFP(T216); lane 6, sfGFP(T216)-PEGMA3; lane 7, sfGFP(S2T216); lane 8, sfGFP(S2T216)-PEGMA3.

(see SI for synthetic procedure). Overall, the molecular weight distribution of the polymers was fairly low, while the crucial presence of the alkyne end-group was confirmed by ^{1}H NMR spectroscopy (see SI, Figures S6 and S7). It should be noted that this CTA was chosen as it bears the alkyne functionality on the R-group, thus permitting the bioconjugation regardless of the thiocarbonylthio bond stability.[92]

Conjugation of the alkyne-functional polymers with the azide-bearing proteins was carried out in Tris buffer solution using copper sulfate as the catalyst, to make a total of nine protein−polymer structures (three sfGFP constructs plus three different polymer molecular weights). Each bioconjugate was then purified by preparative size exclusion chromatography (SEC), which allowed for assessment of the efficiency of the reaction (Figure 3A). When compared to the unmodified sfGFP, all samples were found to exhibit higher molecular weight peaks, eluting at lower volumes, which were attributed to the polymer−protein bioconjugates. It should also be noted that the bioconjugate retention volume decreased with increasing polymer molecular weight, suggesting that higher molecular weight polymers resulted in higher molecular weight bioconjugates. These data confirmed that decoration of site selective sfGFPs with PEGMA polymers of different molecular weights at both positions 2 and 216 was possible.

To confirm the successful formation of the protein−polymer bioconjugates, we next carried out SDS-PAGE analysis on the sfGFP-PEGMA bioconjugates following purification by preparative SEC and sample concentration. Comparison of the unconjugated sfGFP and the product of the CuAAc reactions with the different molecular weight polymers showed that the latter exhibit a significantly broader band at lower mobility, consistent with the presence of the bioconjugate (Figure 3B−D). In the case of PEGMA-1 and PEGMA-2, the broad band with the highest mobility matches that of the neat polymer and is attributed to unreacted polymer chains. This is especially prominent for the PEGMA-1 reactions (Figure 3B), which is due to the fact that removal from the bioconjugate is more challenging for the lowest molecular weight polymer sample. In the case of PEGMA-3, it is hard to determine if there is unconjugated polymer, as the broad polymer band overlaps with the molecular weight assigned to the bioconjugate. However, it was noted that upon heating of these bioconjugate samples, a precipitate was formed which was determined to be unreacted PEGMA (see SI, Figure S8) and hence removal of this by filtration readily allowed for the removal of any unconjugated polymer.

Following production of protein−polymer bioconjugates, we then carried out a series of characterization experiments to assess the impact of conjugation at different sites on the protein surface on the macromolecule properties of the bioconjugates. First, the activity of the protein−polymer bioconjugates was compared with that of the wild type nonconjugated sfGFP, in order to confirm that polymer conjugation does not affect the inherent fluorescence of the protein.[93] To assess activity, we determined the quantum yield of the sfGFP fluorescence before and after conjugation (Figure 4).[94] Using fluorescein free acid as the standard, sfGFP was found to have a quantum yield of 0.613 (±0.016). Similarly, the quantum yield of the bioconjugated sfGFP with PEGMA-2 at the T216 position (sfGFP(T216)-PEGMA2) was found to be 0.638 (±0.014). The comparable quantum yields for the bioconjugate and the sfGFP protein suggest that the fluorophore of the protein is not

DOI: 10.1021/acs.bioconjchem.5b00264
Bioconjugate Chem. 2015, 26, 1890−1899

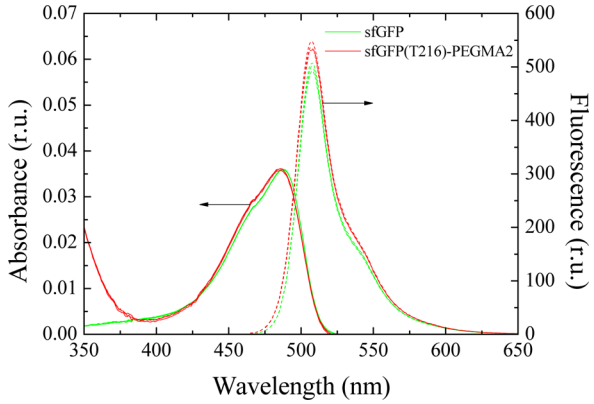

Figure 4. Normalized absorption and fluorescence emission spectra in relative units (r.u.) for the sfGFP and the sfGFP PEGMA-2 bioconjugate with *p*AzF at position T216 (sfGFP(T216)-PEGMA2), showing retention of the protein fluorescence upon conjugation.

affected by polymer conjugation, thus confirming that careful selection of the conjugation site (which is enabled through the site-specific incorporation of a ncAA) allows for the retention of the protein activity. It should be noted that the conjugation did not have an effect on the sfGFP fluorescence even at elevated temperatures, as both the bioconjugate and the wild type sfGFP showed similar fluorescence emissions when cycling the temperature between 25 and 70 °C (see SI, Figure S9). Although we did not test the activity of all the protein−polymer constructs, our data supports an emerging wave of examples showing the ability to maintain protein activity in protein−polymer bioconjugates prepared using site-specifically incorporated ncAAs.[88,93]

We then set out to explore the properties of this series of bioconjugates. First, we wanted to investigate how the conjugation of a temperature-responsive polymer at different residues in the protein affects the overall bioconjugate thermal properties. PEGMA is a temperature-responsive polymer with its transition temperature depending on the PEG side chain length and the overall polymer molecular weight.[89,95] Using turbidimetry, the cloud point of the neat polymers and all nine bioconjugates in Tris buffer was evaluated (Figure 5). As expected due to the hydrophobicity of the polymer end group, the cloud point of the low-molecular-weight PEGMA-1 was at 26.4 °C; however, PEGMA-2 and PEGMA-3 exhibited a hydrophilic−hydrophobic transition at higher temperatures (57.8 and 64.5 °C, respectively).

In the case of the proteins conjugated with PEGMA-1, the cloud point was found to be significantly higher than that of the neat polymer alone, which was attributed to the fact that the protein provides better water solubility than the end group of the polymer itself, thus rendering it more hydrophilic. For the PEGMA-2 and PEGMA-3 bioconjugates, the cloud point was slightly higher than that of the homopolymers. While the transition temperature of the bioconjugates varied from 61 to

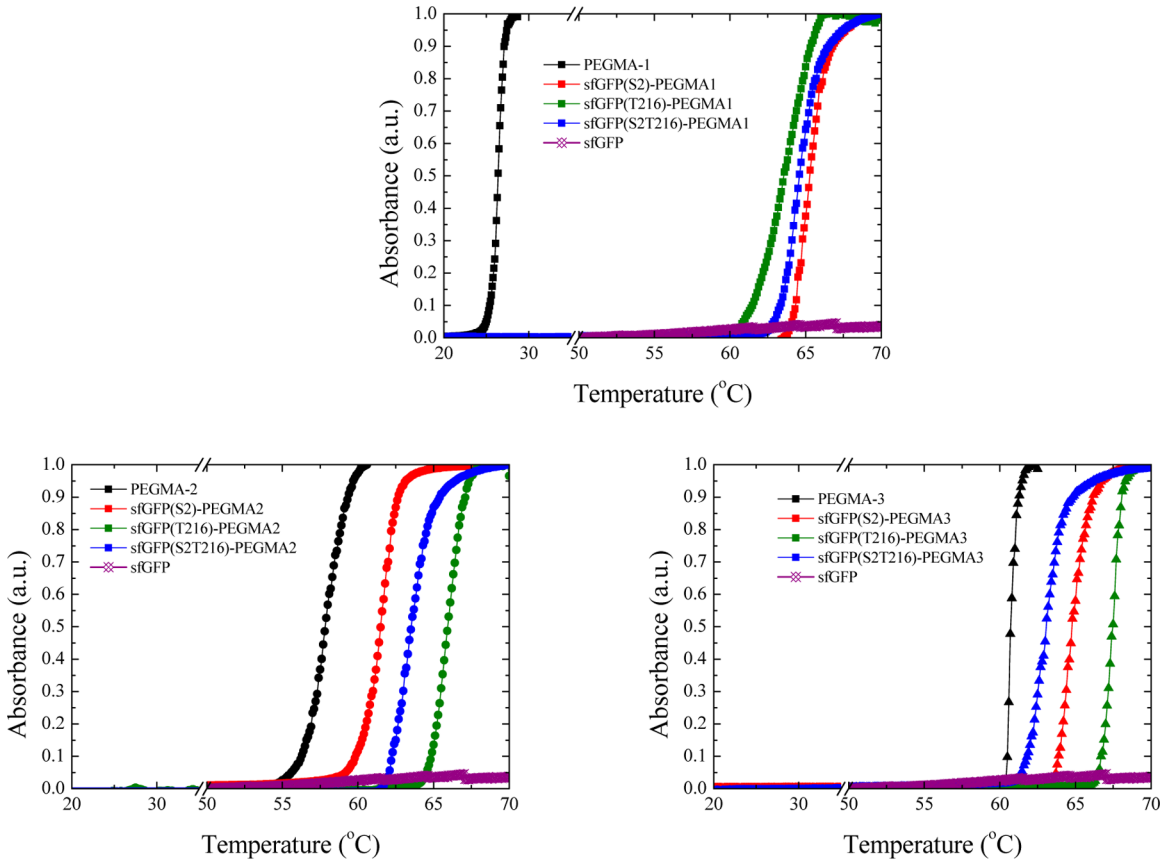

Figure 5. Cloud point curves for the three PEGMA solutions (black lines: squares for PEGMA-1, circles for PEGMA-2, and triangles for PEGMA-3) and their corresponding bioconjugates with the grafting position being sfGFP(S2) (red lines), sfGFP(T216) (green lines), and both sfGFP(S2T216) (blue lines), sfGFP (purple line) are also shown for comparison. Note that all measurements are averages of three runs with a standard deviation of ±1 °C.

DOI: 10.1021/acs.bioconjchem.5b00264
Bioconjugate Chem. 2015, 26, 1890−1899

67 °C there is a distinct effect on the observed transition temperature through variation of the polymer molecular weight and the conjugation site. As such, the shorter polymer (PEGMA-1) results in bioconjugates that regardless of the conjugation site become insoluble at almost the same temperature (63−65 °C). Increasing the molecular weight of the conjugated polymer (PEGMA-2) results in the hybrid that is conjugated at the S2 position (sfGFP(S2)-PEGMA2) to transition at a lower temperature, compared to that conjugated at the T216 position (sfGFP(T216)-PEGMA2) (ca. 4 °C lower). Although both positions are located in the flexible loops of the sfGFP barrel, we suspect that the local environment of conjugation affects the ability of the PEGMA chains to collapse upon heating above their cloud point. This is again observed when comparing the two conjugation sites for the larger (PEGMA-3) polymers (with a ca. 3 °C difference between sfGFP(S2)-PEGMA3 and sfGFP(T216)-PEGMA3). The consistently higher transition temperature for proteins conjugated at the T216 may be attributed to this site being located in a more highly charged region of the protein compared to the S2 site. Note that as expected the higher molecular weight polymer, PEGMA-3, always afforded bioconjugates with higher transition temperatures compared to the PEGMA-2 conjugates.

Interestingly, the transition temperature for the double-conjugated sfGFPs with the PEGMA-1 and PEGMA-2 polymers (sfGFP(S2T216)-PEGMA1 and sfGFP(S2T216)-PEGMA2) occurs at a temperature intermediate to the observed transition of the single modified protein bioconjugates. In contrast, the transition temperature for the higher molecular weight polymer (PEGMA-3) conjugated in two positions (sfGFP(S2T216)-PEGMA3) is slightly lower than that of the two single-functionalized proteins by ca. 1 °C (for sfGFP(S2)-PEGMA3) and 3 °C (for sfGFP(T216)-PEGMA3). This can be attributed to the two polymer chains reaching a critical molecular weight that allows them to interact and thus decrease the effective transition temperature, as seen in other similar bioconjugate systems.[96]

The increase in turbidity and the absence of macroscopic precipitation upon heating the bioconjugates above the transition temperature suggests the formation of dispersed aggregates whereby the hydrophobic part consists of the polymer and the hydrophilic is the protein segment of the bioconjugate. The bioconjugates were thus characterized by dynamic light scattering (DLS) over a range of temperatures (Figure 6), whereby upon heating the hydrodynamic size of the bioconjugates dramatically increased but the unmodified sfGFP retained its original size. This supports the hypothesis that due to the now hydrophobic character of the polymer and the amphiphilic character of the overall hybrid, the bioconjugates self-assemble at elevated temperature. It should however be noted that large aggregate populations were also observed by DLS—regardless of the temperature of the measurement (see SI, Figures S10−S11)—attributed to the presence of aggregates which were also observed in neat buffer. In an attempt to further confirm the formation of bioconjugate assemblies, the heated samples were analyzed by transmission electron microscopy (with the sample preparation taking place at 70 °C, see SI, Figure S12). Unfortunately, only large ill-defined aggregates could be identified which were attributed to the difficulty in sample preparation at elevated temperature.

To gain more information on the solution structure of the protein−polymer bioconjugates, small-angle X-ray scattering (SAXS) experiments were conducted. Data was collected for

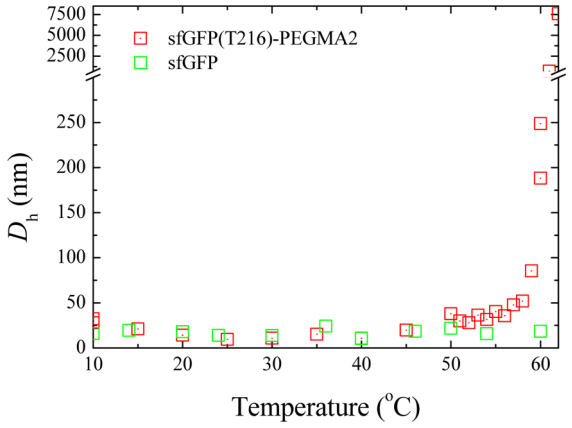

Figure 6. Dependence of the hydrodynamic diameter of sfGFP and the sfGFP(T216)-PEGMA2 bioconjugate on temperature, as determined by DLS analysis.

the sfGFP alone, as well as all the bioconjugates at room and elevated temperature (at 25 and 65 °C). Measurements were performed using dilute solutions (in all cases less than 0.2 mg/mL) to minimize the amount of unwanted aggregation. Fitting analysis (see SI for details) was performed to determine the radius of gyration R_g and shape of the bioconjugate (see Tables S3 and S4). As expected, at 25 °C the bioconjugates all had a larger size than the sfGFP, and furthermore the size of the bioconjugates in solution increased as the molecular weight of the conjugated polymer increased.

A Kratky plot ($q^2I(q)$ vs q) for each sample was derived, from the SAXS data, in order to further analyze the bioconjugate morphology. Such plots are often used to emphasize the differences between compact objects such as globular, structured proteins and that of a random chain, such as an unfolded protein.[97] A bell-shaped curve is obtained in the first case whereas a plateau is found for the second case, and depending on the local rigidity of the chain, an increase in slope as q increases may also be observed.[97] Such a plot however suffers from limitations as it does not allow direct comparison of scattering profiles of objects of different sizes. Moreover, the Kratky plot of partially folded proteins still shows bell-shaped curves owing to the presence of structured regions in the protein. To obviate this problem, a dimensionless Kratky plot was utilized in this work: the intensity $I(q)$ is normalized to the forward scattering intensity $I(0)$, which allows comparison of samples of different molecular weights as $I(0)$ is proportional to the molecular weight; q is normalized to the radius of gyration of the protein, which makes the angular scale independent of the protein size.[98] Analysis of the dimensionless Kratky plots at 25 °C indicated that the conjugation of the polymer does not affect the structured domains of the protein for all of the PEGMA bioconjugates, as the plots at low x-axis values are similar before and after conjugation (see SI, Figure S13). The GFP plots show a symmetrical bell-shaped curve as well as a horizontal asymptote at high x-axis values, characteristic of a folded protein. The presence of more unstructured domains after conjugation is proposed as the plots for the bioconjugates appear to have a higher gradient at high qR_g values ($qR_g > 3$). By SAXS analysis, no significant difference in solution size or shape for the bioconjugates with different site modifications is observed (see SI, Table S3). However, the length of the polymer which is conjugated to the protein has an effect on the solution structure of the resultant bioconjugate, in that the

DOI: 10.1021/acs.bioconjchem.5b00264
Bioconjugate Chem. 2015, 26, 1890−1899

wrapping of the bioconjugated polymers around the protein is more efficient for the longest polymer, PEGMA-3, as observed by an increase of the R_g and a more spherical morphology after bioconjugation (see SI, Table S3).

The dimensionless Kratky plots at elevated temperature 65 °C (close to or above the cloud point of the bioconjugates) show that the sfGFP is equally or more folded in its native form than when it is conjugated to the polymers (see SI, Figure S14). Moreover, the conjugation of the polymers increases the number of unstructured domains as expected for the conjugation of a polymer with a random coil conformation in a collapsed state. The bioconjugates display a more elongated morphology than the sfGFP at elevated temperature. As the sfGFP by itself does not exhibit a more elongated morphology, the elongation is attributed to the polymer chains. This was also confirmed from analysis of the SAXS curves of the polymers at different temperatures (see SI, Figure S15).

In summary, we have shown the successful incorporation of an azide-functional ncAA into sfGFP at multiple locations, synthesizing three sfGFP analogues which could be readily bioconjugated with one or two alkyne-functional PEGMA polymers. Our work described the combination of chemical and biological approaches to produce synthetic protein−polymer bioconjugates having new structures and reversible self-assembly properties. The resulting bioconjugates exhibited no loss in fluorescence, while an increase in temperature resulted in the reversible increase in turbidity of the bioconjugates solutions, suggesting the formation of aggregates. Additionally, the transition temperature was found to be affected by the molecular weight of the polymer as well as the location of the polymer conjugation. Finally, we demonstrated that using the same responsive polymer and conjugating to different sites of a protein leads to no difference in bioconjugate shape, but it does lead to a discernible difference in thermal properties for the bioconjugates. Our work thus highlights that site-selective polymer conjugation, which is possible using protein engineering alongside common conjugation approaches, can be used to fine-tune functional properties of polymer−protein bioconjugates.

Improvements in modified protein yields will open the way to even broader applications. For example, amber suppression technologies *in vivo* are still generally limited to expression of proteins containing ncAAs incorporated into a single instance or few instances within a polypeptide chain.[99,100] New genomically recoded strains[101] lacking release factor 1, cell-free approaches,[75,91,93,102,103] and the ability to site-specifically incorporate multiple types of ncAAs per protein with high efficiencies promise to make possible novel synthesis approaches for unique polymeric materials with atomic-scale resolution over composition, architecture, and functionality.

■ ASSOCIATED CONTENT

Supporting Information

Materials and methods as well as supplementary tables and figures related to the synthesis and characterization of all bioconjugates (PAGE, cloud point, DLS, TEM, SAXS analysis). The Supporting Information is available free of charge on the ACS Publications website at DOI: 10.1021/acs.bioconjchem.5b00264.

■ AUTHOR INFORMATION

Corresponding Authors

*E-mail: m-jewett@northwestern.edu.

*E-mail: r.k.o-reilly@warwick.ac.uk.

Author Contributions

#Dafni Moatsou and Jian Li equally contributed to this work.

Notes

The authors declare no competing financial interest.

■ ACKNOWLEDGMENTS

We acknowledge the EPSRC, University of Warwick, the National Science Foundation (MCB-0943393), the DARPA YFA Program (N66001-11-1-4137), and the NSF Materials Network Grant (DMR - 1108350) for funding. The research leading to these results has received funding from the European Research Council under the European Union's Seventh Framework Programme (FP/2007-2013)/ERC Grant Agreement n. 615142. M.C.J. is a Packard Fellow for Science and Engineering. We thank Tom Lawton with assistance in the preparation of some of the figures.

■ REFERENCES

(1) Abuchowski, A., van Es, T., Palczuk, N. C., and Davis, F. F. (1977) Alteration of immunological properties of bovine serum albumin by covalent attachment of polyethylene glycol. *J. Biol. Chem. 252*, 3578−3581.

(2) Abuchowski, A., McCoy, J. R., Palczuk, N. C., van Es, T., and Davis, F. F. (1977) Effect of covalent attachment of polyethylene glycol on immunogenicity and circulating life of bovine liver catalase. *J. Biol. Chem. 252*, 3582−3586.

(3) Caliceti, P., and Veronese, F. M. (2003) Pharmacokinetic and biodistribution properties of poly(ethylene glycol)−protein conjugates. *Adv. Drug Delivery Rev. 55*, 1261−1277.

(4) Alconcel, S. N. S., Baas, A. S., and Maynard, H. D. (2011) FDA-approved poly(ethylene glycol)-protein conjugate drugs. *Polym. Chem. 2*, 1442−1448.

(5) Fuertges, F., and Abuchowski, A. (1990) The clinical efficacy of poly(ethylene glycol)-modified proteins. *J. Controlled Release 11*, 139−148.

(6) Veronese, F. M. (2001) Peptide and protein PEGylation: a review of problems and solutions. *Biomaterials 22*, 405−417.

(7) Roberts, M. J., Bentley, M. D., and Harris, J. M. (2002) Chemistry for peptide and protein PEGylation. *Adv. Drug Delivery Rev. 54*, 459−476.

(8) Knop, K., Hoogenboom, R., Fischer, D., and Schubert, U. S. (2010) Poly(ethylene glycol) in Drug Delivery: Pros and Cons as Well as Potential Alternatives. *Angew. Chem., Int. Ed. 49*, 6288−6308.

(9) Harris, J. M., and Chess, R. B. (2003) Effect of pegylation on pharmaceuticals. *Nat. Rev. Drug Discovery 2*, 214−221.

(10) Veronese, F. M., and Pasut, G. (2005) PEGylation, successful approach to drug delivery. *Drug Discovery Today 10*, 1451−1458.

(11) Joralemon, M. J., McRae, S., and Emrick, T. (2010) PEGylated polymers for medicine: from conjugation to self-assembled systems. *Chem. Commun. 46*, 1377−1393.

(12) Veronese, F. M., Caliceti, P., and Schiavon, O. (1997) Branched and Linear Poly(Ethylene Glycol): Influence of the Polymer Structure on Enzymological, Pharmacokinetic, and Immunological Properties of Protein Conjugates. *J. Bioact. Compat. Polym. 12*, 196−207.

(13) Pelegri-O'Day, E. M., Lin, E.-W., and Maynard, H. D. (2014) Therapeutic Protein−Polymer Conjugates: Advancing Beyond PEGylation. *J. Am. Chem. Soc. 136*, 14323−14332.

(14) Cobo, I., Li, M., Sumerlin, B. S., and Perrier, S. (2015) Smart hybrid materials by conjugation of responsive polymers to biomacromolecules. *Nat. Mater. 14*, 143−159.

(15) Gil, E. S., and Hudson, S. M. (2004) Stimuli-reponsive polymers and their bioconjugates. *Prog. Polym. Sci. 29*, 1173−1222.

(16) Stayton, P. S., Shimoboji, T., Long, C., Chilkoti, A., Ghen, G., Harris, J. M., and Hoffman, A. S. (1995) Control of protein-ligand recognition using a stimuli-responsive polymer. *Nature 378*, 472−474.

DOI: 10.1021/acs.bioconjchem.5b00264
Bioconjugate Chem. 2015, 26, 1890−1899

(17) Krishna, O. D., and Kiick, K. L. (2010) Protein- and peptide-modified synthetic polymeric biomaterials. *Pept. Sci. 94*, 32−48.
(18) Dirks, A. J., Nolte, R. J. M., and Cornelissen, J. J. L. M. (2008) Protein−Polymer Hybrid Amphiphiles. *Adv. Mater. 20*, 3953−3957.
(19) Velonia, K. (2010) Protein-polymer amphiphilic chimeras: recent advances and future challenges. *Polym. Chem. 1*, 944−952.
(20) Hoffman, A. S., and Stayton, P. S. (2007) Conjugates of stimuli-responsive polymers and proteins. *Prog. Polym. Sci. 32*, 922−932.
(21) Hoffman, A. S., and Stayton, P. S. (2004) Bioconjugates of smart polymers and proteins: synthesis and applications. *Macromol. Symp. 207*, 139−152.
(22) Borner, H. G., and Schlaad, H. (2007) Bioinspired functional block copolymers. *Soft Matter 3*, 394−408.
(23) Li, H., Li, M., Yu, X., Bapat, A. P., and Sumerlin, B. S. (2011) Block copolymer conjugates prepared by sequentially grafting from proteinsvia RAFT. *Polym. Chem. 2*, 1531−1535.
(24) Boyer, C., Bulmus, V., Liu, J., Davis, T. P., Stenzel, M. H., and Barner-Kowollik, C. (2007) Well-Defined Protein−Polymer Conjugates via in Situ RAFT Polymerization. *J. Am. Chem. Soc. 129*, 7145−7154.
(25) Chen, G., and Hoffman, A. S. (1993) Preparation and properties of thermoreversible, phase-separating enzyme-oligo(N-isopropylacrylamide) conjugates. *Bioconjugate Chem. 4*, 509−514.
(26) Ding, Z., Chen, G., and Hoffman, A. S. (1996) Synthesis and Purification of Thermally Sensitive Oligomer−Enzyme Conjugates of Poly(N-isopropylacrylamide)−Trypsin. *Bioconjugate Chem. 7*, 121−125.
(27) Bulmus, V., Ding, Z., Long, C. J., Stayton, P. S., and Hoffman, A. S. (1999) Site-Specific Polymer−Streptavidin Bioconjugate for pH-Controlled Binding and Triggered Release of Biotin. *Bioconjugate Chem. 11*, 78−83.
(28) Ding, Z., Long, C. J., Hayashi, Y., Bulmus, E. V., Hoffman, A. S., and Stayton, P. S. (1999) Temperature Control of Biotin Binding and Release with A Streptavidin-Poly(N-isopropylacrylamide) Site-Specific Conjugate. *Bioconjugate Chem. 10*, 395−400.
(29) Fong, R. B., Ding, Z., Long, C. J., Hoffman, A. S., and Stayton, P. S. (1999) Thermoprecipitation of Streptavidin via Oligonucleotide-Mediated Self-Assembly with Poly(N-isopropylacrylamide). *Bioconjugate Chem. 10*, 720−725.
(30) Le Droumaguet, B., Mantovani, G., Haddleton, D. M., and Velonia, K. (2007) Formation of giant amphiphiles by post-functionalization of hydrophilic protein-polymer conjugates. *J. Mater. Chem. 17*, 1916−1922.
(31) Hannink, J. M., Cornelissen, J. J. L. M., Farrera, J. A., Foubert, P., De Schryver, F. C., Sommerdijk, N. A. J. M., and Nolte, R. J. M. (2001) Protein−Polymer Hybrid Amphiphiles. *Angew. Chem., Int. Ed. 40*, 4732−4734.
(32) Dirks, A. J., van Berkel, S. S., Hatzakis, N. S., Opsteen, J. A., van Delft, F. L., Cornelissen, J. J. L. M., Rowan, A. E., van Hest, J. C. M., Rutjes, F. P. J. T., and Nolte, R. J. M. (2005) Preparation of biohybrid amphiphiles via the copper catalysed Huisgen [3 + 2] dipolar cycloaddition reaction. *Chem. Commun.*, 4172−4174.
(33) Maeda, H. (2001) SMANCS and polymer-conjugated macromolecular drugs: advantages in cancer chemotherapy. *Adv. Drug Delivery Rev. 46*, 169−185.
(34) Boerakker, M. J., Hannink, J. M., Bomans, P. H. H., Frederik, P. M., Nolte, R. J. M., Meijer, E. M., and Sommerdijk, N. A. J. M. (2002) Giant Amphiphiles by Cofactor Reconstitution. *Angew. Chem., Int. Ed. 41*, 4239−4241.
(35) Velonia, K., Rowan, A. E., and Nolte, R. J. M. (2002) Lipase Polystyrene Giant Amphiphiles. *J. Am. Chem. Soc. 124*, 4224−4225.
(36) Ding, Z., Chen, G., and Hoffman, A. S. (1998) Unusual properties of thermally sensitive oligomer−enzyme conjugates of poly(N-isopropylacrylamide)−trypsin. *J. Biomed. Mater. Res. 39*, 498−505.
(37) Shimoboji, T., Larenas, E., Fowler, T., Kulkarni, S., Hoffman, A. S., and Stayton, P. S. (2002) Photoresponsive polymer−enzyme switches. *Proc. Natl. Acad. Sci. U.S.A. 99*, 16592−16596.
(38) Taniguchi, M., Kobayashi, M., and Fujii, M. (1989) Properties of a reversible soluble−insoluble cellulase and its application to repeated hydrolysis of crystalline cellulose. *Biotechnol. Bioeng. 34*, 1092−1097.
(39) Tae Gwan, P., and Hoffman, A. S. (1993) Synthesis and characterization of a soluble, temperature-sensitive polymer-conjugated enzyme. *J. Biomater. Sci., Polym. Ed. 4*, 493−504.
(40) Boerakker, M. J., Botterhuis, N. E., Bomans, P. H. H., Frederik, P. M., Meijer, E. M., Nolte, R. J. M., and Sommerdijk, N. A. J. M. (2006) Aggregation Behavior of Giant Amphiphiles Prepared by Cofactor Reconstitution. *Chem.—Eur. J. 12*, 6071−6080.
(41) Reynhout, I. C., Cornelissen, J. J. L. M., and Nolte, R. J. M. (2007) Self-Assembled Architectures from Biohybrid Triblock Copolymers. *J. Am. Chem. Soc. 129*, 2327−2332.
(42) Li, M., De, P., Gondi, S. R., and Sumerlin, B. S. (2008) Responsive Polymer-Protein Bioconjugates Prepared by RAFT Polymerization and Copper-Catalyzed Azide-Alkyne Click Chemistry. *Macromol. Rapid Commun. 29*, 1172−1176.
(43) Tao, L., Mantovani, G., Lecolley, F., and Haddleton, D. M. (2004) α-Aldehyde Terminally Functional Methacrylic Polymers from Living Radical Polymerization: Application in Protein Conjugation "Pegylation. *J. Am. Chem. Soc. 126*, 13220−13221.
(44) Lecolley, F., Tao, L., Mantovani, G., Durkin, I., Lautru, S., and Haddleton, D. M. (2004) A new approach to bioconjugates for proteins and peptides ("pegylation") utilising living radical polymerisation. *Chem. Commun.*, 2026−2027.
(45) Heredia, K. L., Bontempo, D., Ly, T., Byers, J. T., Halstenberg, S., and Maynard, H. D. (2005) In Situ Preparation of Protein−"Smart" Polymer Conjugates with Retention of Bioactivity. *J. Am. Chem. Soc. 127*, 16955−16960.
(46) Gilmore, J. M., Scheck, R. A., Esser-Kahn, A. P., Joshi, N. S., and Francis, M. B. (2006) N-Terminal Protein Modification through a Biomimetic Transamination Reaction. *Angew. Chem., Int. Ed. 45*, 5307−5311.
(47) Dixon, H. B. F. (1984) N-terminal modification of proteins—a review. *J. Protein Chem. 3*, 99−108.
(48) Chilkoti, A., Chen, G., Stayton, P. S., and Hoffman, A. S. (1994) Site-Specific Conjugation of a Temperature-Sensitive Polymer to a Genetically Engineered Protein. *Bioconjugate Chem. 5*, 504−507.
(49) Shimoboji, T., Ding, Z., Stayton, P. S., and Hoffman, A. S. (2001) Mechanistic Investigation of Smart Polymer−Protein Conjugates. *Bioconjugate Chem. 12*, 314−319.
(50) Ding, Z., Fong, R. B., Long, C. J., Stayton, P. S., and Hoffman, A. S. (2001) Size-dependent control of the binding of biotinylated proteins to streptavidin using a polymer shield. *Nature 411*, 59−62.
(51) Schoffelen, S., van Eldijk, M. B., Rooijakkers, B., Raijmakers, R., Heck, A. J. R., and van Hest, J. C. M. (2011) Metal-free and pH-controlled introduction of azides in proteins. *Chem. Sci. 2*, 701−705.
(52) Lutz, J.-F., and Börner, H. G. (2008) Modern trends in polymer bioconjugates design. *Prog. Polym. Sci. 33*, 1−39.
(53) Heredia, K. L., and Maynard, H. D. (2007) Synthesis of protein-polymer conjugates. *Org. Biomol. Chem. 5*, 45−53.
(54) Johnson, R. P., John, J. V., and Kim, I. (2013) Recent developments in polymer−block−polypeptide and protein−polymer bioconjugate hybrid materials. *Eur. Polym. J. 49*, 2925−2948.
(55) Boyer, C., Huang, X., Whittaker, M. R., Bulmus, V., and Davis, T. P. (2011) An overview of protein-polymer particles. *Soft Matter 7*, 1599−1614.
(56) Canalle, L. A., Lowik, D. W. P. M., and van Hest, J. C. M. (2010) Polypeptide-polymer bioconjugates. *Chem. Soc. Rev. 39*, 329−353.
(57) Nicolas, J., Mantovani, G., and Haddleton, D. M. (2007) Living Radical Polymerization as a Tool for the Synthesis of Polymer-Protein/Peptide Bioconjugates. *Macromol. Rapid Commun. 28*, 1083−1111.
(58) Le Droumaguet, B., and Nicolas, J. (2010) Recent advances in the design of bioconjugates from controlled/living radical polymerization. *Polym. Chem. 1*, 563−598.

DOI: 10.1021/acs.bioconjchem.5b00264
Bioconjugate Chem. 2015, 26, 1890−1899

(59) Broyer, R. M., Grover, G. N., and Maynard, H. D. (2011) Emerging synthetic approaches for protein-polymer conjugations. *Chem. Commun. 47*, 2212−2226.
(60) Klok, H.-A. (2005) Biological−synthetic hybrid block copolymers: Combining the best from two worlds. *J. Polym. Sci., Part A: Polym. Chem. 43*, 1−17.
(61) Thordarson, P., Le Droumaguet, B., and Velonia, K. (2006) Well-defined protein−polymer conjugates—synthesis and potential applications. *Appl. Microbiol. Biotechnol. 73*, 243−254.
(62) Gauthier, M. A., and Klok, H.-A. (2008) Peptide/protein-polymer conjugates: synthetic strategies and design concepts. *Chem. Commun.*, 2591−2611.
(63) Borchmann, D. E., Carberry, T. P., and Weck, M. (2014) "Bio"-Macromolecules: Polymer-Protein Conjugates as Emerging Scaffolds for Therapeutics. *Macromol. Rapid Commun. 35*, 27−43.
(64) Oshiba, Y., Tamaki, T., Ohashi, H., Hirakawa, H., Yamaguchi, S., Nagamune, T., and Yamaguchi, T. (2013) Effect of length of molecular recognition moiety on enzymatic activity switching. *J. Biosci. Bioeng. 116*, 433−437.
(65) Kochendoerfer, G. G., Chen, S.-Y., Mao, F., Cressman, S., Traviglia, S., Shao, H., Hunter, C. L., Low, D. W., Cagle, E. N., Carnevali, M., et al. (2003) Design and Chemical Synthesis of a Homogeneous Polymer-Modified Erythropoiesis Protein. *Science 299*, 884−887.
(66) Dumas, A., Lercher, L., Spicer, C. D., and Davis, B. G. (2015) Designing logical codon reassignment - Expanding the chemistry in biology. *Chem. Sci. 6*, 50−69.
(67) Wang, L., and Schultz, P. G. (2005) Expanding the Genetic Code. *Angew. Chem., Int. Ed. 44*, 34−66.
(68) Wang, P., Tang, Y., and Tirrell, D. A. (2003) Incorporation of Trifluoroisoleucine into Proteins in Vivo. *J. Am. Chem. Soc. 125*, 6900−6906.
(69) Tang, Y., Wang, P., Van Deventer, J. A., Link, A. J., and Tirrell, D. A. (2009) Introduction of an Aliphatic Ketone into Recombinant Proteins in a Bacterial Strain that Overexpresses an Editing-Impaired Leucyl-tRNA Synthetase. *ChemBioChem 10*, 2188−2190.
(70) Johnson, J. A., Lu, Y. Y., Van Deventer, J. A., and Tirrell, D. A. (2010) Residue-specific incorporation of non-canonical amino acids into proteins: recent developments and applications. *Curr. Opin. Chem. Biol. 14*, 774−780.
(71) Tang, Y., and Tirrell, D. A. (2002) Attenuation of the Editing Activity of the Escherichia coli Leucyl-tRNA Synthetase Allows Incorporation of Novel Amino Acids into Proteins in Vivo. *Biochemistry 41*, 10635−10645.
(72) Kiick, K. L., Saxon, E., Tirrell, D. A., and Bertozzi, C. R. (2002) Incorporation of azides into recombinant proteins for chemoselective modification by the Staudinger ligation. *Proc. Natl. Acad. Sci. U.S.A. 99*, 19−24.
(73) Liu, C. C., and Schultz, P. G. (2010) Adding New Chemistries to the Genetic Code. *Annu. Rev. Biochem. 79*, 413−444.
(74) Chin, J. W. (2014) Expanding and Reprogramming the Genetic Code of Cells and Animals. *Annu. Rev. Biochem. 83*, 379−408.
(75) Hong, S. H., Kwon, Y.-C., and Jewett, M. C. (2014) Non-standard amino acid incorporation into proteins using Escherichia coli cell-free protein synthesis. *Front. Chem. 2*, DOI: 10.3389/fchem.2014.00034.
(76) O'Donoghue, P., Ling, J., Wang, Y.-S., and Soll, D. (2013) Upgrading protein synthesis for synthetic biology. *Nat. Chem. Biol. 9*, 594−598.
(77) Kolb, H. C., Finn, M. G., and Sharpless, K. B. (2001) Click Chemistry: Diverse Chemical Function from a Few Good Reactions. *Angew. Chem., Int. Ed. 40*, 2004−2021.
(78) Rostovtsev, V. V., Green, L. G., Fokin, V. V., and Sharpless, K. B. (2002) A Stepwise Huisgen Cycloaddition Process: Copper(I)-Catalyzed Regioselective "Ligation" of Azides and Terminal Alkynes. *Angew. Chem., Int. Ed. 41*, 2596−2599.
(79) Huisgen, R. (1963) 1,3-Dipolar Cycloadditions. Past and Future. *Angew. Chem., Int. Ed. 2*, 565−598.
(80) Huisgen, R. (1963) Kinetics and Mechanism of 1,3-Dipolar Cycloadditions. *Angew. Chem., Int. Ed. 2*, 633−645.
(81) Schoffelen, S., Lambermon, M. H. L., Eldijk, M. B. v., and Hest, J. C. M. v. (2008) Site-Specific Modification of Candida antarctica Lipase B via Residue-Specific Incorporation of a Non-Canonical Amino Acid. *Bioconjugate Chem. 19*, 1127−1131.
(82) Reddington, S. C., Tippmann, E. M., and Dafydd Jones, D. (2012) Residue choice defines efficiency and influence of bioorthogonal protein modification via genetically encoded strain promoted Click chemistry. *Chem. Commun. 48*, 8419−8421.
(83) Peeler, J. C., Woodman, B. F., Averick, S., Miyake-Stoner, S. J., Stokes, A. L., Hess, K. R., Matyjaszewski, K., and Mehl, R. A. (2010) Genetically Encoded Initiator for Polymer Growth from Proteins. *J. Am. Chem. Soc. 132*, 13575−13577.
(84) Bulmus, V. (2011) RAFT polymerization mediated bioconjugation strategies. *Polym. Chem. 2*, 1463−1472.
(85) Longo, J., Yao, C., Rios, C., Chau, N. T. T., Boulmedais, F., Hemmerle, J., Lavalle, P., Schiller, S. M., Schaaf, P., and Jierry, L. (2015) Reversible biomechano-responsive surface based on green fluorescent protein genetically modified with unnatural amino acids. *Chem. Commun. 51*, 232−235.
(86) Lavigueur, C., Garcia, J. G., Hendriks, L., Hoogenboom, R., Cornelissen, J. J. L. M., and Nolte, R. J. M. (2011) Thermoresponsive giant biohybrid amphiphiles. *Polym. Chem. 2*, 333−340.
(87) Xia, Y., Tang, S., and Olsen, B. D. (2013) Site-specific conjugation of RAFT polymers to proteins via expressed protein ligation. *Chem. Commun. 49*, 2566−2568.
(88) Averick, S., Karácsony, O., Mohin, J., Yong, X., Moellers, N. M., Woodman, B. F., Zhu, W., Mehl, R. A., Balazs, A. C., Kowalewski, T., et al. (2014) Cooperative, Reversible Self-Assembly of Covalently Pre-Linked Proteins into Giant Fibrous Structures. *Angew. Chem., Int. Ed. 53*, 8050−8055.
(89) Lutz, J.-F. (2008) Polymerization of oligo(ethylene glycol) (meth)acrylates: Toward new generations of smart biocompatible materials. *J. Polym. Sci., Part A: Polym. Chem. 46*, 3459−3470.
(90) Young, T. S., Ahmad, I., Yin, J. A., and Schultz, P. G. (2010) An Enhanced System for Unnatural Amino Acid Mutagenesis in E. coli. *J. Mol. Biol. 395*, 361−374.
(91) Hong, S. H., Kwon, Y.-C., Martin, R. W., Des Soye, B. J., de Paz, A. M., Swonger, K. N., Ntai, I., Kelleher, N. L., and Jewett, M. C. (2015) Improving Cell-Free Protein Synthesis through Genome Engineering of Escherichia coli Lacking Release Factor 1. *ChemBioChem 16*, 844−853.
(92) De, P., Li, M., Gondi, S. R., and Sumerlin, B. S. (2008) Temperature-Regulated Activity of Responsive Polymer−Protein Conjugates Prepared by Grafting-from via RAFT Polymerization. *J. Am. Chem. Soc. 130*, 11288−11289.
(93) Albayrak, C., and Swartz, J. R. (2014) Direct Polymerization of Proteins. *ACS Synth. Biol. 3*, 353−362.
(94) Würth, C., Grabolle, M., Pauli, J., Spieles, M., and Resch-Genger, U. (2013) Relative and absolute determination of fluorescence quantum yields of transparent samples. *Nat. Protoc. 8*, 1535−1550.
(95) Bebis, K., Jones, M. W., Haddleton, D. M., and Gibson, M. I. (2011) Thermoresponsive behaviour of poly[(oligo(ethyleneglycol methacrylate)]s and their protein conjugates: importance of concentration and solvent system. *Polym. Chem. 2*, 975−982.
(96) Liu, M., Tirino, P., Radivojevic, M., Phillips, D. J., Gibson, M. I., Leroux, J.-C., and Gauthier, M. A. (2013) Molecular Sieving on the Surface of a Protein Provides Protection Without Loss of Activity. *Adv. Funct. Mater. 23*, 2007−2015.
(97) Receveur-Brechot, V., and Durand, D. (2012) How Random are Intrinsically Disordered Proteins? A Small Angle Scattering Perspective. *Curr. Protein Pept. Sci. 13*, 55−75.
(98) Durand, D., Vivès, C., Cannella, D., Pérez, J., Pebay-Peyroula, E., Vachette, P., and Fieschi, F. (2010) NADPH oxidase activator p67phox behaves in solution as a multidomain protein with semi-flexible linkers. *J. Struct. Biol. 169*, 45−53.

DOI: 10.1021/acs.bioconjchem.5b00264
Bioconjugate Chem. 2015, 26, 1890−1899

(99) O'Donoghue, P., Ling, J., Wang, Y. S., and Söll, D. (2013) Upgrading protein synthesis for synthetic biology. *Nat. Chem. Biol. 9*, 594−8.
(100) Li, X., and Liu, C. C. (2014) Biological Applications of Expanded Genetic Codes. *ChemBioChem. 15*, 2335−2341.
(101) Lajoie, M. J., Rovner, A. J., Goodman, D. B., Aerni, H.-R., Haimovich, A. D., Kuznetsov, G., Mercer, J. A., Wang, H. H., Carr, P. A., Mosberg, J. A., et al. (2013) Genomically Recoded Organisms Expand Biological Functions. *Science 342*, 357−360.
(102) Hong, S. H., Ntai, I., Haimovich, A. D., Kelleher, N. L., Isaacs, F. J., and Jewett, M. C. (2014) Cell-free Protein Synthesis from a Release Factor 1 Deficient Escherichia coli Activates Efficient and Multiple Site-specific Nonstandard Amino Acid Incorporation. *ACS Synth. Biol. 3*, 398−409.
(103) Hong, S. H., Kwon, Y.-C., Martin, R. W., Des Soye, B. J., de Paz, A. M., Swonger, K. N., Ntai, I., Kelleher, N. L., and Jewett, M. C. (2015) Improving Cell-Free Protein Synthesis through Genome Engineering of Escherichia coli Lacking Release Factor 1. *ChemBioChem 16*, 844−853.

DOI: 10.1021/acs.bioconjchem.5b00264
Bioconjugate Chem. 2015, 26, 1890−1899

Self-assembly of temperature-responsive protein-polymer bioconjugates

Dafni Moatsou,† Jian Li,‡ Arnaz Ranji,‡ Anaïs Pitto-Barry,† Ioanna Ntai,‡ Michael C. Jewett,‡* Rachel K. O'Reilly†*

Supporting Information

1. Materials and Methods

2. Supplementary Characterization Tables and Figures

Fluorescence of the sfGFP-dye bioconjugates

PAGE analysis of sfGFP-dye(1) bioconjugates

LC-MS of sfGFP-dye(1) bioconjugates

MS of sfGFP modified with *p*AzF and the sfGFP-dye(1) bioconjugate

SEC chromatograms of the alkyne-functional polymers

Materials and Methods

Chemicals: 2,2′-Azobis(2-methylpropionitrile) (AIBN) was recrystallized from methanol and stored at 4 ºC. Poly(ethylene glycol) methyl ether methacrylate ($OEGMA_{300}$) was purchased from Sigma-Aldrich and was passed through a basic alumina plug before use. All other chemicals were purchased from Sigma-Aldrich and used without further purification. In all experiments a pH 8 Tris-Cl buffer was used. The protease inhibitor cocktail was purchased from Thermo Scientific, Strep-tag® Purification Columns were obtained from IBA GmbH, Goettingen, Germany. Spin filters (MWCO 10 kDa) were obtained from Fisher Scientific.

Synthesis of N-(6-(diethylamino)-9-(2-((prop-2-yn-1-yloxy)carbonyl)phenyl)-3H-xanthen-3-ylidene)-N-ethylethanaminium (dye (1)).

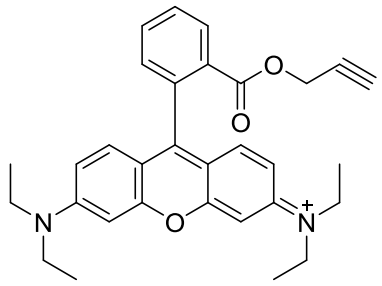

dye(**1**)

In an ice cold round-bottom flask propargyl alcohol (81 µL, 1.392 mmol, 1 eq.), rhodamine B (1g, 2.088 mmol, 1.5 eq.), *N*,*N*'-dicyclohexylcarbodiimide (310.2 mg, 1.503 mmol, 1.08 eq.) were dissolved in 50 mL dichloromethane (CH_2Cl_2) before the addition of 4-(dimethylamino)pyridine (11.1 mg, 0.090 mmol, 0.065 eq.). The reaction was allowed to warm to room temperature and was stirred overnight. The precipitates were removed by filtration and the solvent was removed under reduced pressure. The product, dye (**1**), was isolated as a dark purple-green solid after purification by column chromatography (382 mg, 57% isolated yield). TLC analysis (CH_2Cl_2:methanol 9:1): R_f = 0.43; ^{1}H NMR (300 MHz, $CDCl_3$): δ (ppm) 8.29 (m, 1H, Ar), 7.80 (m, 1H, Ar), 7.72 (m, 1H, Ar), 7.31 (m, 1H, Ar), 7.03 (d, *J* = 9.5 Hz, 2H, Ar), 6.87 (dd, *J* = 2.4, 9.5 Hz, 2H, Ar), 6.80 (d, *J* = 2.4 Hz, 2H, Ar), 4.59 (d, *J* = 2.4, 1H, -OCH_2-), 3.57-3.65 (q, *J* = 7.1 Hz, 8H, C**H**$_2$-CH_3), 2.39 (t, *J* = 2.4 Hz,

1H, C≡CH), 1.29 (t, *J* = 7.1 Hz, 12H, CH_3); ^{13}C NMR (125 MHz, MeOD): δ (ppm) 113.7, 112.9, 95.8, 76.3, 75.3, 52.3, 45.6, 12.1; HRMS (m/z): expected, 481.2486; found, 481.2492 $[M]^+$.

Synthesis of prop-2-yn-1-yl 2-phenyl-2-((phenylcarbonothioyl)thio)acetate (2).

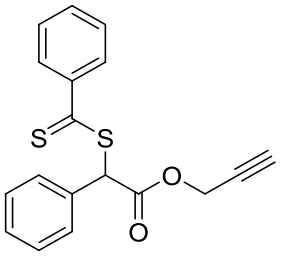

2

The synthesis of the alkyne chain transfer agent (CTA) was concluded in 3 steps, based on procedures from the literature.[1] For the first step, α-bromophenyl acetic acid (5g, 23.25 mmol, 1 eq.) was added to thionyl chloride (12.6 mL, 172.81 mmol, 7.4 eq.) and the mixture was refluxed under nitrogen for 2.5 hours. Excess reagents and by-products were removed by distillation at room temperature to yield a brown oil that was used without further purification.

For the second step, in a dry round bottom flask, propargyl alcohol (6.77 mL, 116.21 mmol, 5 eq.) and triethylamine (6.48 mL, 46.5 mmol, 2 eq.) were dissolved in dry dichloromethane (25 mL) and purged with nitrogen before the brown oil was added dropwise. The mixture was stirred overnight before washing with 0.1M HCl, followed by water, then saturated $NaHCO_3$, and finally again with water. The organic layer was then dried over $MgSO_4$. The pure product prop-2-yn-1-yl 2-bromo-2-phenylacetate was isolated by flash chromatography (2.8 g, 48% isolated yield). TLC (CH_2Cl_2:Pet Ether): R_f = 0.73; ^{1}H NMR (300 MHz, $CDCl_3$): δ (ppm) 7.39 (m, 2H, Ar), 7.24 (m, 3H, Ar), 5.25 (d, *J* = 2.5 Hz, 1H, -C**H**-Br), 4.61 (m, -O-C**H_2**-, 2H), 2.36 (m, 1H, ≡CH); ^{13}C NMR (75 MHz, $CDCl_3$): δ (ppm) 167.6, 135.3, 129.5, 128.7, 128.0, 76.5, 75.9, 53.7, 45.9.

For the third step,[2] phenyl magnesium bromide (3M solution in diethyl ether, 2.95 mL, 8.84 mmol, 1 eq.) was added to a dry round bottom flask containing dry THF (9 mL). The mixture was heated to 40 ºC before the slow addition of carbon disulfide (532 µL, 8.84 mmol, 1 eq.). Then, the previously synthesized prop-2-yn-1-yl 2-bromo-2-phenylacetate (2.35 g, 9.29 mmol, 1.05 eq.) was added and the

reaction was allowed to proceed overnight at 80 ºC. Upon cooling down, 20 mL of ice-cold water was added and the organic layer was extracted with diethyl ether three times. The combined ether phases were washed with water and dried over $MgSO_4$. The product was purified by flash chromatography (1.33g, 46% isolated yield). TLC (Et_2O:Pet ether 1:2): R_f = 0.54; ^{11}H NMR (300 MHz, $CDCl_3$) δ (ppm) 7.98 (dd, *J* = 1.1, 8.4 Hz, Ar, 2H), 7.44 (m, Ar, 8H), 5.71 (s, -S-CH-, 1H), 4.74 (m, CH_2, 2H), 2.47 (d, *J* = 2.5, ≡CH, 1H); ^{13}C NMR (125 MHz, MeOD) δ (ppm) 226.3, 168.1, 143.9, 132.7, 132.6, 129.0, 128.9, 128.6, 128.5, 128.3, 76.6, 45.5, 58.5, 53.0; HRMS (m/z): expected, 349.0327; found, 349.0325 $[M+Na]^+$.

Synthesis of alkyne-functional poly[(oligo ethylene glycol) methyl ether methacrylate] (PEGMA). For a typical polymerization, AIBN (1.2 mg, 7 μmol, 0.1 eq.), **2** (22.8 mg, 70μmol, 1 eq.), and the monomer $OEGMA_{300}$ (2 mL, 7 mmol, 100 eq.) were dissolved in dioxane (4 mL) and degassed by three freeze-pump-thaw cycles. The ampoule was then charged with nitrogen and the reaction was stirred for three hours at 65 ºC. The polymer was isolated *via* precipitation in cold hexane, followed by dialysis against pure water to remove excess monomer.

Table S1. Reagent quantities and conditions used for the synthesis of the alkyne-functional polymers PEGMA-1, PEGMA-2, and PEGMA-3.

		PEGMA-1	PEGMA-2	PEGMA-3
$OEGMA_{300}$	m (g)	2.0	1.0	2.0
	n (mmol)	6.670	3.334	6.670
	eq.	50	50	100
2	m (mg)	43.2	21.6	22.8
	n (mmol)	0.132	0.066	0.070
	eq.	1	1	1
AIBN	m (mg)	2.2	1.1	1.2
	n (mmol)	0.013	0.007	0.007
	eq.	0.1	0.1	0.1
dioxane	V (mL)	4	2	4
time	(h)	2	2.5	3

Protein expression, purification, and mass spectrometry analysis.

The super folder green fluorescent protein (sfGFP) construct was that reported by Hong.[3] The sequence encoding the sfGFP variant is shown here (with the S2 and T216 highlighted in red):

M S K G E E L F T G V V P I L V E L D G
D V N G H K F S V R G E G E G D A T I G
K L T L K F I C T T G K L P V P W P T L
V T T L T Y G V Q C F S R Y P D H M K R
H D F F K S A M P E G Y V Q E R T I S F
K D D G K Y K T R A V V K F E G D T L V
N R I E L K G T D F K E D G N I L G H K
L E Y N F N S H N V Y I T A D K Q K N G
I K A N F T V R H N V E D G S V Q L A D
H Y Q Q N T P I G D G P V L L P D N H Y
L S T Q T V L S K D P N E K G T R D H M
V L H E Y V N A A G I T W S H P Q F E K

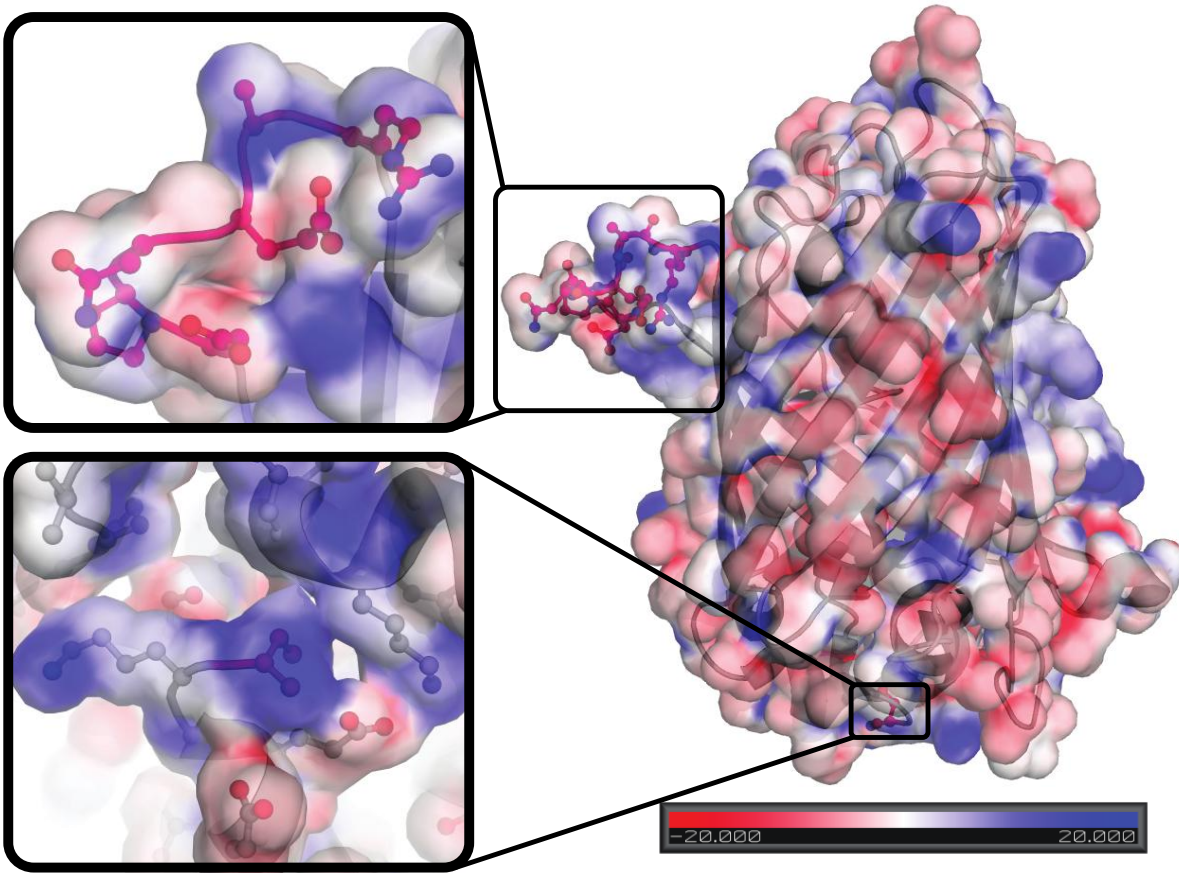

Figure S1. Surface charge of sfGFP calculated using APBS and rendered in PyMol. Residues 210-215 displayed in top left panel in pink with spheres. Serine 2 displayed in bottom panel in pink. Surfaces are displayed as 40% opaque. Blue color: Positive charge; Red color: Negative charge. Based on the surface Figure, we can conclude that T216 site is more accessible than S2 site. Please note that the Figure is generated based on the original sfGFP amino acid sequence (PDB:2B3P), not our currently used sfGFP (which has 2 further amino acids G and T inserted between the K216 and

R215 sites). Therefore the original site R215 becomes current site R217. The inserted G is now at site 215 and T is at the site 216.

To incorporate the non-natural amino acid *p*-azidophenylalanine (*p*AzF) into the super folder green fluorescent protein (sfGFP), *E. coli* BL21(DE3) cells were co-transformed with the pEVOL-*p*AzF plasmid that encodes the aminoacyl-tRNA synthetase/suppressor tRNA pair[4] and the appropriate mutant pY71-sfGFP plasmid (pY71-sfGFP-S2TAG, pY71-sfGFP-T216TAG or pY71-sfGFP-S2TAG/T216TAG). All sfGFP mutants were C-terminally Strep-tagged for purification. Cells were grown overnight at 37 °C in 20 mL LB medium supplemented with chloramphenicol (34 μg/mL) and kanamycin (50 μg/mL). Of the overnight culture, 15 mL was used to inoculate 500 mL of LB in a 2.5-L flask containing appropriate antibiotics. After incubation at 37 °C and 250 rpm for 1 h, 5 mL of *p*AzF (500 mM) was added to the culture given a final concentration of 5 mM. After 30 min, protein expression was induced by addition of arabinose and IPTG to final concentrations of 0.1% and 5 mM, respectively. After overnight induction, cells were harvested by centrifugation at 6,000 g and 4 °C for 15 min. The cell pellets were washed once with 20 mL phosphate buffered saline (PBS buffer, pH 7.4) and then centrifuged at 5,000 g and 4 °C for 10 min. The washed pellets were resuspended in 4 mL of PBS buffer plus 50 μL protease inhibitor cocktail and lysed on ice by sonication for three pulses (50% amplitude, 45 s on and 59 s off). The lysate was clarified by centrifugation for 10 min at 12,000 g and 4 °C. Proteins were purified from the supernatant by 1-mL Strep-tag® Purification Columns according to the manufacture's protocol. Purified proteins were analyzed by 4-12% NuPAGE SDS-PAGE gels. Yields of purified proteins were determined by the Quick-Start Bradford Protein Assay Kit (Bio-Rad).

The purified and modified proteins were analysed by LC-MS using a 100 mm × 75 μm ID PLRP-S column in-line with an Orbitrap Elite (ThermoFisher, Waltham, MA). All MS methods included the following events: 1) FT scan, m/z 400−2,000, 120,000 resolving power and 2) data-dependent MS/MS on the top 2 peaks in each spectrum from scan event 1 using higher-energy collisional dissociation (HCD) with normalized collision energy of 25, isolation width 50 m/z, and detection of

ions with resolving power of 60,000. All data were analyzed using QualBrowser, part of the Xcalibur software packaged with the ThermoFisher Orbitrap Elite.

Conjugation of dye(1) with sfGFP-azide to yield the sfGFP-dye(1) bioconjugates. In a typical reaction 250 μL of the mono-azide functional sfGFP solution (1.125 mg, 41.7 nmol) was stirred overnight with 250 μL of a freshly prepared Tris buffer solution containing the dye(**1**) (0.216 mg, 0.416 μmol, 10 eq.), tris-(hydroxypropyltriazolylmethyl)amine (THPTA) (0.905 mg, 2.08 μmol, 50 eq.), (+)-sodium L-ascorbate (4.13 mg, 20.83 μmol, 500 eq.), and $CuSO_4 \cdot 5H_2O$ (0.104 mg, 0.42 μmol, 10 eq.). Excess dye was then removed by consecutive spin filtration-addition of fresh buffer cycles until the filtrate was clear. For conjugation of the dye(**1**) to the di-azide functional sfGFP, all reagents were doubled in quantity.

Conjugation of PEGMA with sfGFP-azide to yield the sfGFP-PEGMA bioconjugate. In a typical reaction 200 μL of the mono-azide functional sfGFP solution (0.878 mg, 32.5 nmol) were stirred overnight with 200 μL of a freshly prepared buffer solution containing PEGMA-1 (24.8 mg, 3.25 μmol, 100 eq.), tris-(hydroxypropyltriazolylmethyl)amine (THPTA) (0.706 mg, 1.63 μmol, 50 eq.), (+)-sodium L-ascorbate (3.2 mg, 16.26 μmol, 500 eq.), and $CuSO_4 \cdot 5H_2O$ (0.081 mg, 0.33 μmol, 10 eq.). For conjugation of PEGMA to the di-azide functional sfGFP, all reagents were doubled in quantity. The pure bioconjugates were isolated initially by SEC in order to remove low molecular weight impurities and excess sfGFP. Excess polymer was then removed by thermal precipitation.

Analytical methods for characterizing protein, polymers, and the bioconjugates. Nuclear magnetic resonance (^{1}H and ^{13}C NMR) spectra were recorded on a Bruker AC-250, a Bruker DPX-300, a Bruker AV-400 or a Bruker DPX- 400, a Bruker AV-500, and a Bruker AV II-700 spectrometer. Chemical shifts are reported as δ in parts per million (ppm) and referenced to the chemical shift of the residual solvent resonances ($CDCl_3$ ^{1}H: δ = 7.26 ppm; ^{13}C: δ = 77.2 ppm; MeOD ^{1}H: δ = 4.78 ppm, ^{13}C: δ = 49.3 ppm). High resolution mass spectra (HRMS) were collected using a Bruker MaXis UHR-ESITOF. Dynamic light scattering measurements were conducted on a Malvern Zetasizer equipped with a 632 nm laser source and a fixed angle detector (172 ^{o}) and analysed using v6.20

software. Aqueous size exclusion chromatography was performed on a GE Healthcare AKTA-Purifier equipped with a HiLoad Superdex 75 PG column and a fraction collector, operating at 4 ºC. SEC measurements were carried out on an Agilent 390-MDS equipped with differential refractive index and UV detectors. The separation was achieved by a guard column (Varian PLGel 5 μm) and two mixed-D columns (Varian PLGel 5 μm) using THF (2% TEA mixture) as the eluent at a flow rate of 1 mL/min. Data analysis was performed using Cirrus v3.3 with calibration curves produced using Varian Polymer laboratories Easi-Vials linear poly(methyl methacrylate) standards. Fluorescence spectra were recorded on a single beam Perkin Elmer LS55 fluorometer. UV/vis spectroscopy was carried out on a Perkin Elmer Lambda 35 UV/vis spectrometer, equipped with a PTP-1+1 Peltier temperature programmer. For the cloud point measurements the absorbance of the samples at λ = 600 nm was measured as a function of the solution temperature. Each sample was measured three times. Transmission electron microscopy was performed on a JEOL 2000FX in bright field mode. The samples were prepared as follows: the bioconjugates were diluted 100 fold in buffer and heated to 75 ºC on a hot plate before deposition of 4 μL onto a graphene oxide TEM grid (also heated to 75ºC before deposition of the sample droplet). After the drop dried, the grid was rinsed five times with pre-heated deionized water to remove buffer salts before allowing cooling down.

Supplementary Characterization Tables and Figures

Table S2. Monoisotopic masses of sfGFP species calculated from mass spectrometric data. Masses calculated from MS data are marked as "experimental", while masses calculated based on the sequence of the proteins are marked as "theoretical". The start (*N*-terminal) methionine of sfGFP is usually cleaved post-translationally by methionine aminopeptidase present in the *E. coli* proteome. However, the presence of an unnatural amino acid at S2, appears to hinder this enzyme.

GFP species	**Mass (Da, Experimental)**	**Mass (Da, Theoretical)**	**error (ppm)**	**Shift from WT-sfGFP (Da, Experimental)**	**Shift from WT-sfGFP (Da, Theoretical)**
WT-sfGFP[a]	26847.52	26847.45	2.6	--	--
sfGFP(T216)-*p*AzF[a]	26934.57	25934.47	3.5	87.12	87.02
sfGFP(S2)-*p*AzF	27079.67	27079.53	5.1	232.22[b]	232.08[b]
sfGFP(S2T216)-*p*AzF	27166.67	27166.55	4.3	319.22[b]	319.10[b]

[a]start methionine has been cleaved
[b]mass shift includes the mass of the start methionine residue (131.0405Da)

Fluorescence of the sfGFP-dye bioconjugates

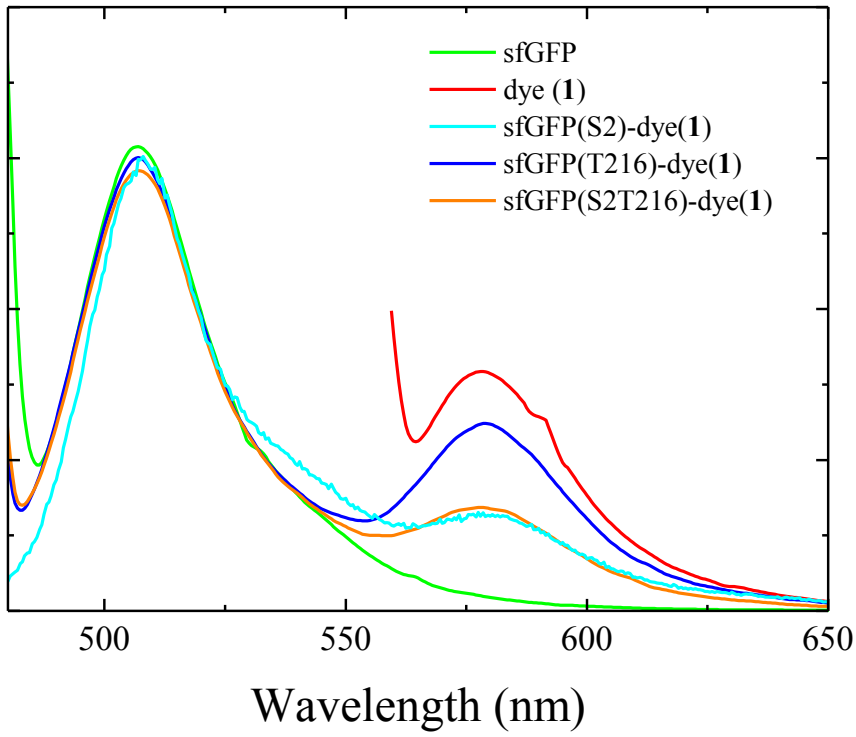

Figure S2. Fluorescence emission spectra for the native sfGFP and the three sfGFP-dye(1) bioconjugates excited at 470 nm, and free dye(1) excited at 550 nm. After extensive purification of the three dye-coupled protein samples, they were examined by fluorescence and the intrinsic activity, as indicated by the protein fluorescence, was preserved. As expected, when excited at 470 nm the anticipated emission maximum at 507 nm was observed and in addition, a new emission peak at 580 nm was also observed, attributed to the bioconjugated rhodamine moiety.

PAGE analysis of sfGFP-dye(1) bioconjugates

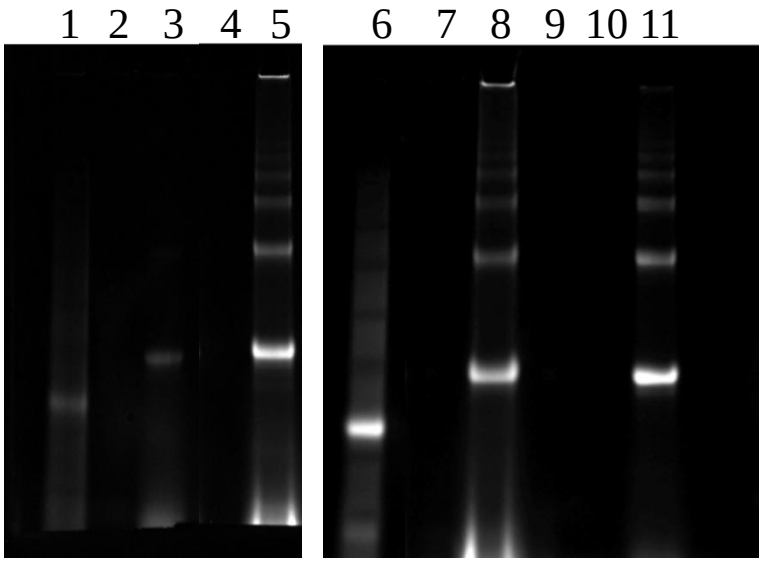

Figure S3. PAGE gel of the protein-dye bioconjugates visualized by ruby red fluorescence: lane 1 – ladder, lane 2 – wtsfGFP, lane 3 – wtsfGFP mixed with dye(**1**), lane 4 – sfGFP(T216), lane 5 – sfGFP(T216)-dye(**1**), lane 6 – ladder, lane 7 – sfGFP(S2), lane 8 – sfGFP(S2)-dye(**1**), lane 9 – blank, lane 10 – sfGFP(S2T216), lane 11 – sfGFP(S2T216)-dye(**1**).

LC-MS of sfGFP-dye(1) bioconjugates

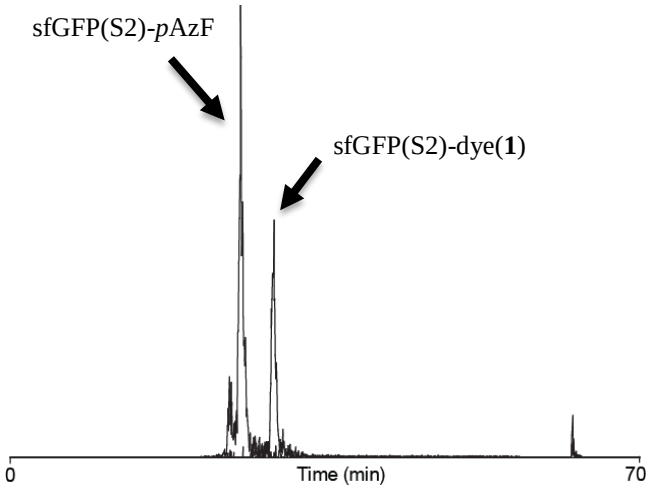

Figure S4. LC-MS of the sfGFP(S2)-dye(1) bioconjugate. The successful conjugation of the dye onto the protein species was also confirmed by LC-MS whereby a new peak at higher retention times was observed.

MS of sfGFP modified with *p*AzF and the sfGFP-dye(1) bioconjugate

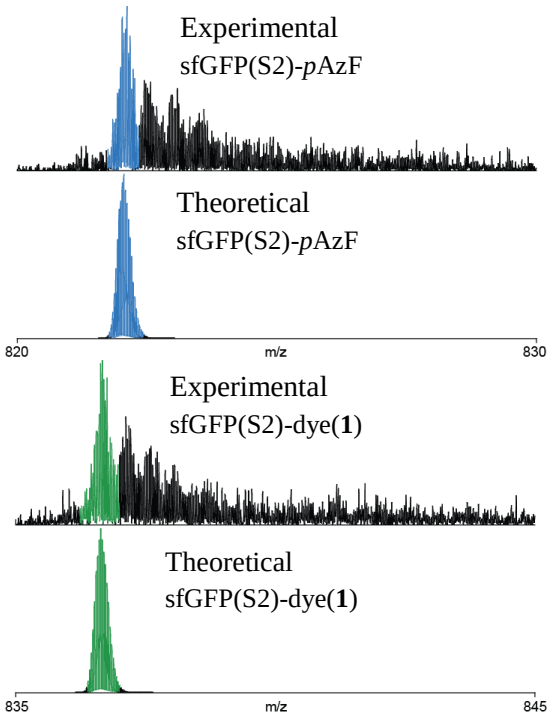

Figure S5. Mass spectra of the sfGFP modified with *p*AzF at position S2 (sfGFP(S2)-*p*AzF), and the corresponding GFP-dye bioconjugate (sfGFP(S2)-dye(**1**)). Major peaks in each spectrum coincide with the theoretical peaks for each species and have been highlighted. Smaller peaks to the right of the major peaks are due to oxidation of the protein—a common electrochemical reaction occurring during electrospray ionization. The theoretical mass distribution of the functionalized protein matches the experimental, thus confirming the presence of the protein-dye bioconjugate and therefore the accessibility of the S2 residue towards conjugation.

SEC chromatograms of the alkyne-functional polymers

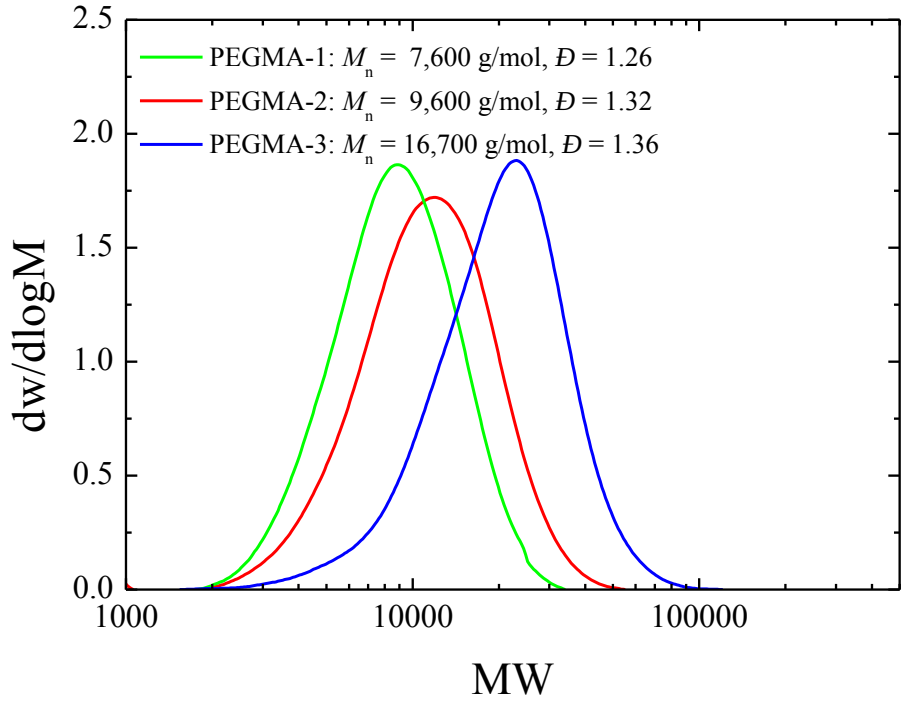

Figure S6. SEC chromatograms (THF (2% triethylamine) with PMMA standards) for the three alkyne-functional polymers (green: PEGMA-1, red: PEGMA-2, blue: PEGMA-3)

^{1}H NMR spectroscopy of the alkyne-functional polymer

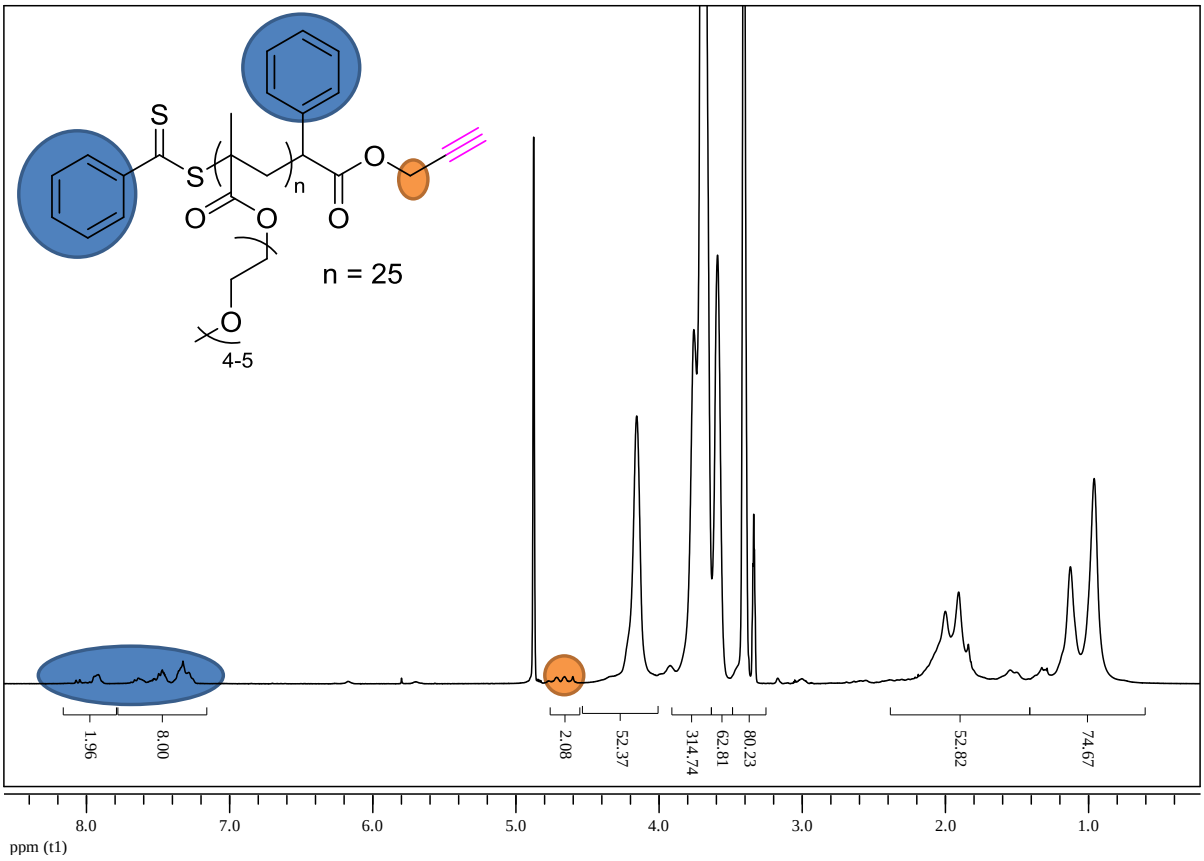

Figure S7. 1H NMR spectrum of PEGMA-1 in MeOD showing the characteristic signals for the corresponding highlighted end-group protons. While the alkyne proton signal was not visible, as it overlapped with the polymer repeat unit signals, the integration comparison of the aromatic protons (at ca. 8.2 ppm) and the CH_2 next to the alkyne (at ca. 4.7 ppm) suggests the presence of the alkyne end group in each of the polymer samples.

Purification of the bioconjugates / removal of excess polymer

For the purification of the bioconjugates and the removal of excess polymer, the solutions were heated to 70 ºC and the green-cloudy supernatant was isolated and used for further analyses. The pink precipitate was isolated and found to be PEGMA homopolymer by ^{1}H NMR spectroscopy.

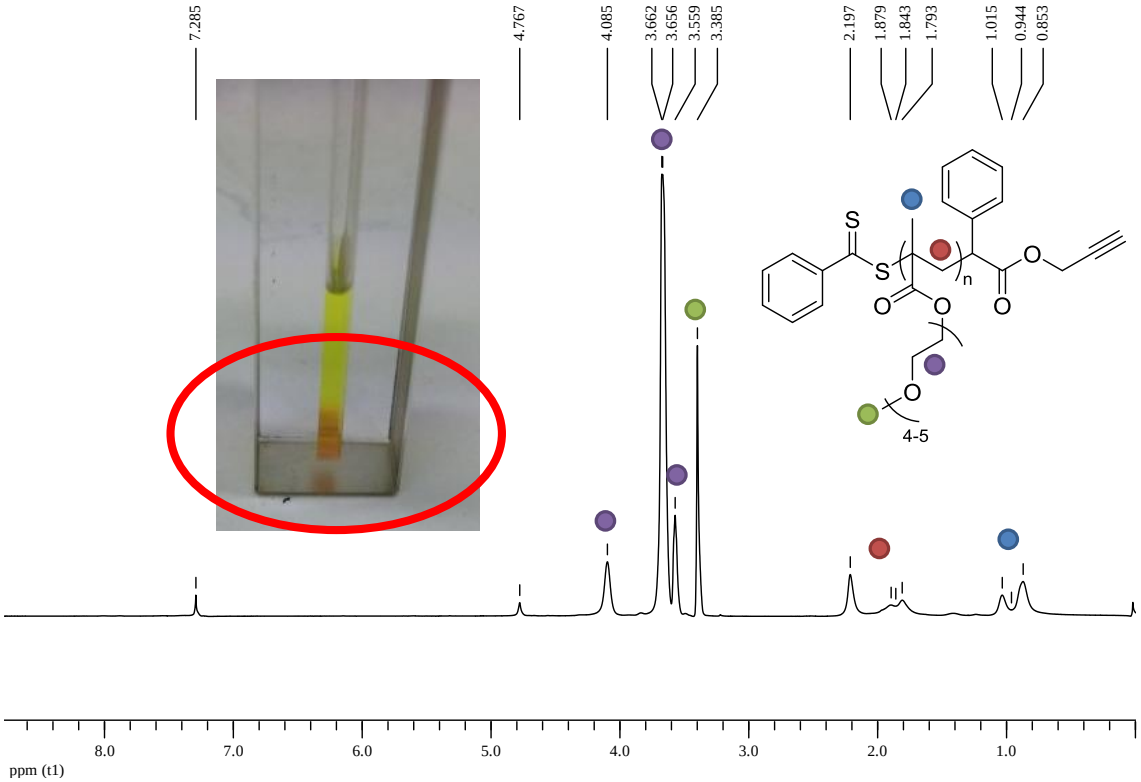

Figure S8. Photograph showing the observed pink precipitate and the corresponding ^{1}H NMR spectrum, highlighting the characteristic peaks of the PEGMA homopolymer, which was isolated following slow heating of the bioconjugate solution.

Fluorescence cycling with temperature

The effect of increased temperature on the bioconjugates was also examined by measuring the fluorescence intensity upon heating to 70 ºC. At elevated temperature the unmodified sfGFP and the sfGFP(T216)-PEGMA2 bioconjugate fluorescence (Figure S9) had significantly decreased, however, upon re-cooling to room temperature the initial fluorescence was almost completely regained in both cases. After multiple heating-cooling cycles, the emission intensity had significantly dropped for both samples; however in the case of the bioconjugate the drop was more prominent. This may be attributed to the fact that upon heating the polymer becomes hydrophobic, creating a hydrophobic environment on the surface of the protein that was previously hydrophilic, thus disrupting the protein folding and resulting in the loss of fluorescence upon repeated temperature cycling. It is noteworthy that this effect is only significant after six heating cycles (that correspond to ~ 1 hour total heating).

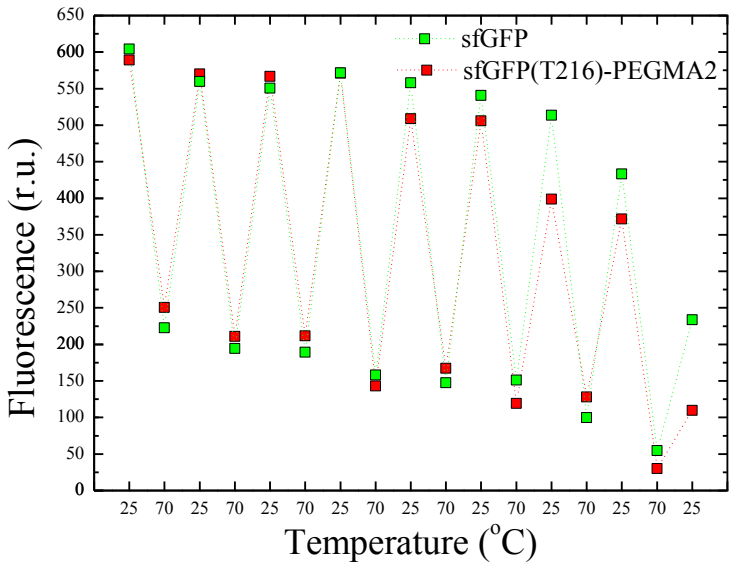

Figure S9. Plot of the fluorescence maxima intensity (λ_{ex} = 470 nm, λ_{em} = 507 nm) of the unmodified sfGFP and the sfGFP(T216)-PEGMA2 bioconjugate as a function of temperature upon multiple heating-cooling cycles.

Turbidimetry studies of the polymer and bioconjugates cloud point

300 µL of the bioconjugate solution was diluted with an equal amount of Tris buffer before placing in a UV cuvette. The sample absorption at 600 nm was measured while increasing the temperature using a 1 ºC/min ramp. Each sample was measured three times and the individual runs were averaged.

Characterization of the bioconjugates by DLS and TEM analysis

Dynamic light scattering (DLS) measurements

For the determination of the hydrodynamic size of the proteins and the bioconjugates, 10 µL of the solution was diluted with 2 mL of buffer or water. The measurements were recorded in triplicate at temperatures ranging from 5-70 ºC. Due to the scattering of the buffer, the results were analyzed by fitting of a stretch exponential decay function to the correlation function and elimination of the processes corresponding to the buffer scattering.[5] In order to confirm the outcome, the measurements were repeated in water with no corrections. While the number-based size distributions only showed small particles, large aggregates were still observable in the intensity-based distributions.

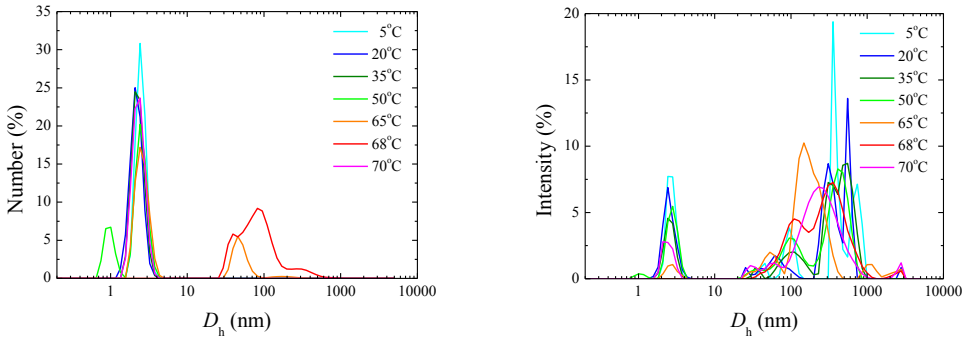

Figure S10. Size distributions by number (left) and intensity (right) for the sfGFP(T216)-PEGMA2 bioconjugate at different temperatures.

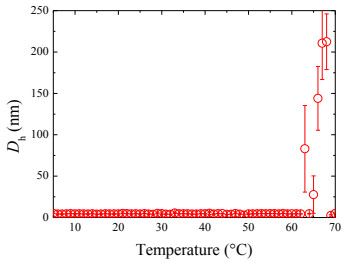

Figure S11. Hydrodynamic diameters (number averaged) of the sfGFP(T216)-PEGMA2 bioconjugate as a function of temperature, measured in water.

TEM imaging of the bioconjugates at elevated temperatures

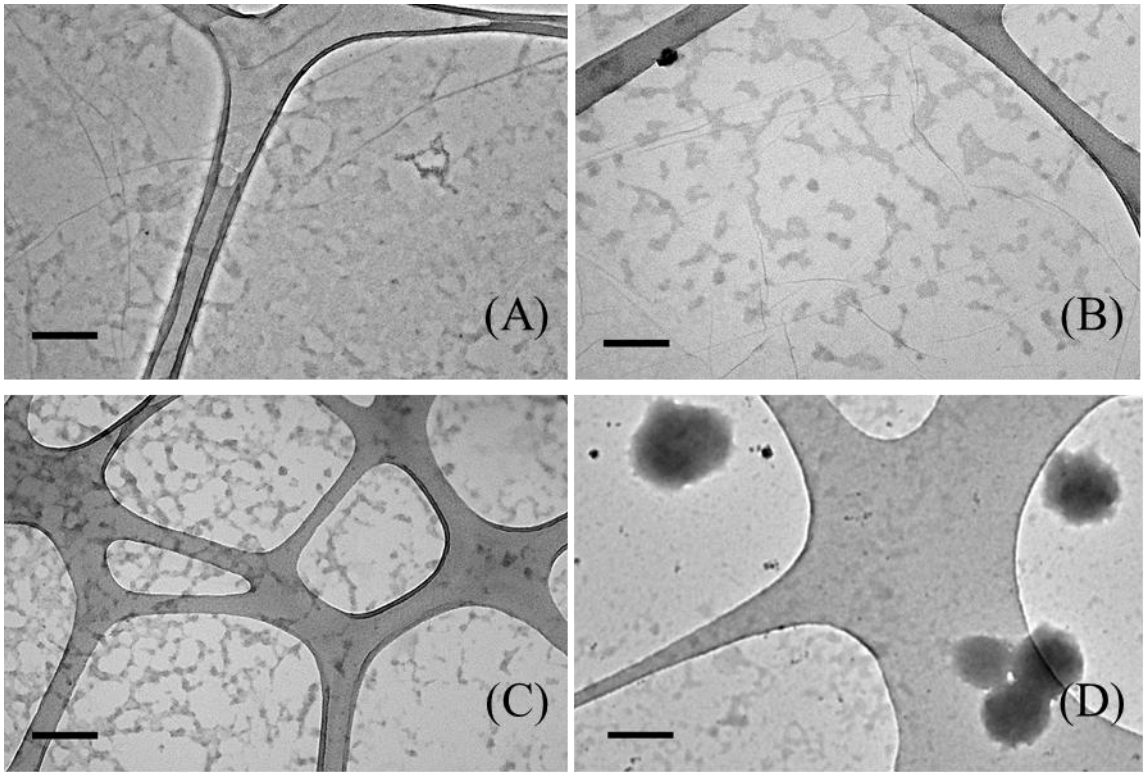

Figure S12. TEM images of the sfGFP(S2)-PEGMA1 bioconjugate (A), sfGFP(S2)-PEGMA2 bioconjugate (B), and sfGFP(S2)-PEGMA3 bioconjugate (C), as well as the bifunctional sfGFP(S2T216)-PEGMA2 bioconjugate (D) prepared at temperatures above the cloud point of the bioconjugates. The bioconjugates were imaged on graphene oxide grids without staining (Scale bars: 200 nm).[6]

To examine the size and shape of the aggregates, a small sample was deposited on a TEM grid at elevated temperature in order for the structures to retain their formation. Figure S12 (A-C) shows

representative images from the sfGFP(S2)-polymer bioconjugates with all three PEGMAs. The presence of self-assembled structures at elevated temperatures further confirms the amphiphilic character of the bioconjugates at elevated temperatures. In addition, analysis of the double conjugated sgGFP(S2T216)-PEGMA2 by TEM (Figure S12D) indicates that larger particles (up to 400 nm) in addition to the smaller aggregates are present in solution at elevated temperature. This can be attributed to the higher polymer content in the double conjugate, and thus higher hydrophobic content of the bioconjugate. While the shape of the aggregates varies from spherical to lamellar, across the series of conjugates with different PEGMA lengths, we hypothesized these observations may be due to the challenging nature of the sample preparation at elevated temperature rather than an actual difference in morphology.

Characterization of the bioconjugates by small-angle X-ray scattering

Small-angle X-ray scattering (SAXS) measurements were carried out on the SAXS/WAXS beam line at the Australian Synchrotron facility at a photon energy of 11 keV. The samples were prepared in 18.2 MΩ cm water and were run using a well-plate and a 1.5 mm diameter quartz capillary. The well-plate and the capillary were held in a sample holder with temperature control achieved via a water bath connected to the sample holder. The measurements were collected at a sample to detector distance of 3.252 m to give a q range of 0.005 to 0.3 $Å^{-1}$, where q is the scattering vector and is related to the scattering angle (2θ) and the photon wavelength (λ) by the following equation:

$$q = \frac{4\pi \sin(\theta)}{\lambda}$$

All patterns were normalised to fixed transmitted flux using a quantitative beam stop detector. The scattering from a blank (Tris buffer) was measured in the same location as sample collection and was subtracted for each measurement. The two-dimensional SAXS images were converted to one-dimensional SAXS profile ($I(q)$ *versus* q) by circular averaging, where $I(q)$ is the scattering intensity. Both Igor with the NCNR analysis macro[7] and Primus[8] were used to analyse the data. This was

performed by using the Guinier law.[9] At low q values ($qR_g < 1.3$), Ln $I(q)$ varies linearly as a function of q^2 with a slope equal to $R_g^2/3$. Moreover such a plot also extrapolates an estimation of the intensity at the origin $I(0)$. Values of R_g were determined using two different software programs, with one also providing information on the general shape of the structure with the use of a dimension parameter, s (a value of 0 indicates a sphere whereas a value closer to 1 indicates an elongated morphology).[9,10]

Table S3. SAXS analyses results for the sfGFP-PEGMA bioconjugates at 25 ºC.

	Native sfGFP	**S2**	**T216**	**S2T216**
	R_g = 2.1 nm s = 0.31	-	-	-
PEGMA-1	R_g = 1.4 nm s = n/a[a]	R_g = 2.0 nm s = 0.13	R_g = 2.5 nm s = 0.10	R_g = 2.2 nm s = 0.19
PEGMA-2	R_g = 1.5 nm s = 0.15	R_g = 2.6 nm s = 0.09	R_g = 2.3 nm s = 0.14	n/a
PEGMA-3	R_g = 1.2 nm s = 0.16	R_g = 2.9 nm s = 0.21	R_g = 3.1 nm s = 0.16	R_g = 3.2 nm s = 0.17

[a] Aggregation is observed and thus the calculation of the radius of gyration was not possible.

Table S4. SAXS analyses results for the sfGFP-PEGMA bioconjugates at 65 ºC.

	Native sfGFP	**S2**	**T216**	**S2T216**
No polymer	R_g = 2.1 nm s = 0.24	-	-	-
PEGMA-1	R_g = 1.7 nm s = 0.19	R_g = 2.2 nm s = 0.29[a]	R_g = 2.2 nm s = 0.36[a]	R_g = 2.3 nm s = 0.42[a]
PEGMA-2	R_g = 1.7 nm s = 0.11	n/a	R_g = 2.3 nm s = n/a[a]	n/a
PEGMA-3	R_g = 1.8 nm s = 0.05	R_g = 2.5 nm s = 0.30[a]	R_g = 2.5 nm s = 0.33[a]	R_g = 2.7 nm s = 0.15

[a] Aggregation is observed and thus the calculation of the radius of gyration was not possible.

All protein bioconjugates display similar or higher R_g than the native sfGFP, as well as smaller s parameter, which indicates some sort of coiling of the polymer around the protein at 25 ºC and the formation of a more spherical morphology. At elevated temperature, 65 ºC, all protein bioconjugates display higher R_g than the sfGFP and higher s parameter; this indicates that the bioconjugate morphology is more elongated with the bioconjugation. The R_g also tends to increase for all sites of conjugation when the molecular weight of the polymer increases for both temperatures. The S2T216 protein-conjugates surprisingly does not show an obvious increase of R_g compared to the single site protein-conjugate, which may indicate that complete double conjugation may not occur. This is in good correlation with the PAGE results (Figure 3).

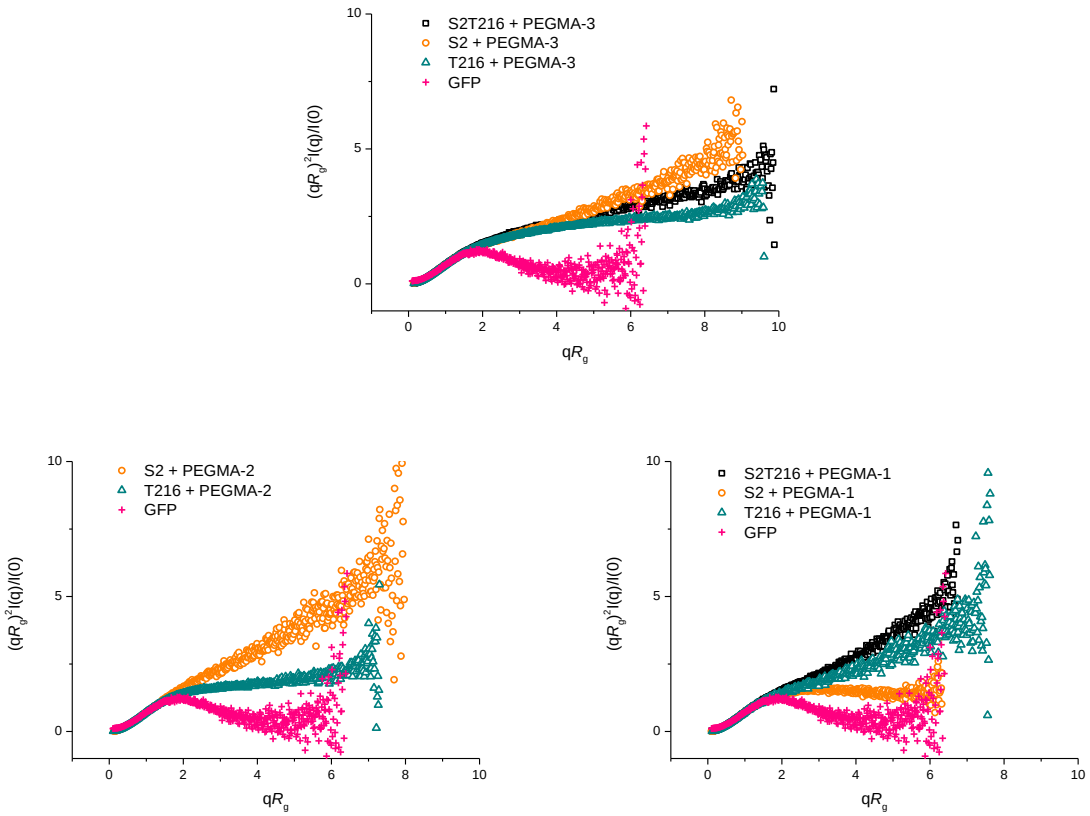

Figure S13. Selected dimensionless Kratky plots at 25 °C.

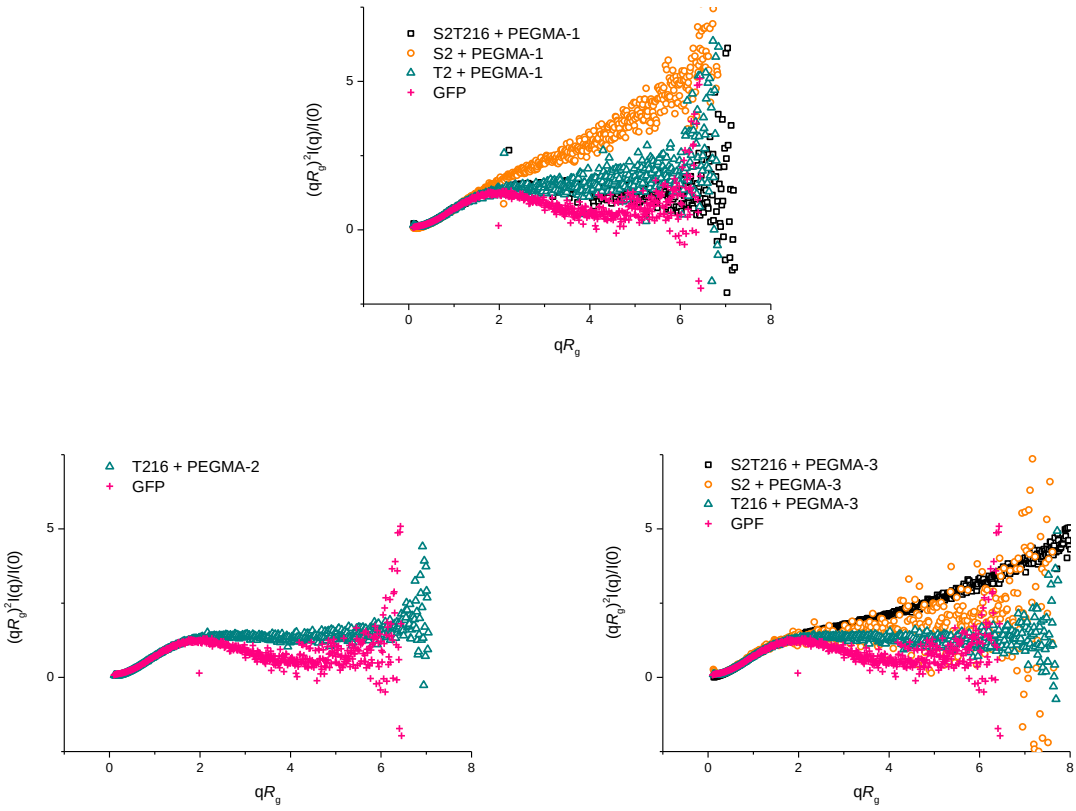

Figure S14. Selected dimensionless Kratky plots at 65 °C.

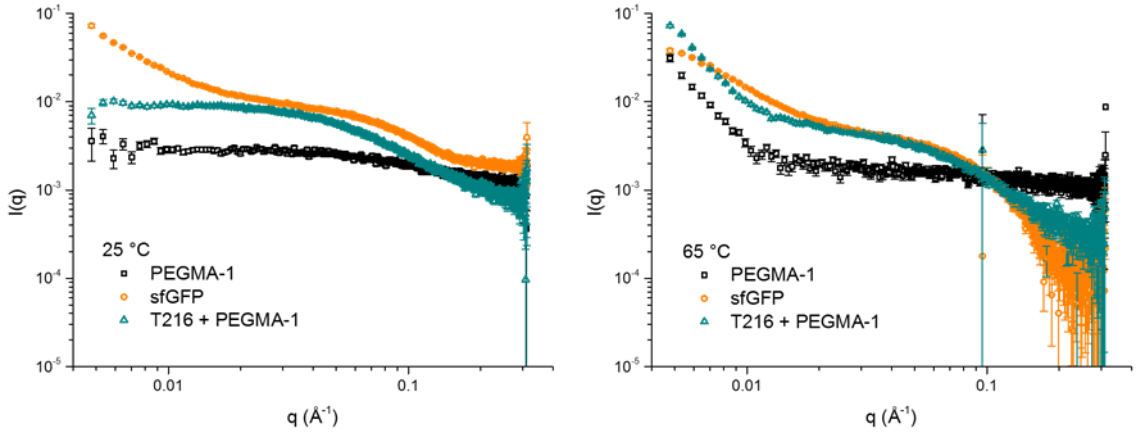

Figure S15. SAXS curves for PEGMA-1, native sfGPF and bioconjugate T216 + PEGMA-1 at 25 and 65 °C. An important change of shape is observed for the PEGMA-1 data at low q values for the different temperature, which indicates aggregation. Almost no change of shape is observed for the sfGPF data at low q values at different temperature. A strong upturn is observed at low q values for the bioconjugate depending on the temperature.

References

(1) Blakey, I.; Schiller, T. L.; Merican, Z.; Fredericks, P. M. *Langmuir* 2009, *26*, 692-701.
(2) Perrier, S.; Takolpuckdee, P.; Westwood, J.; Lewis, D. M. *Macromolecules* 2004, *37*, 2709-2717.
(3) Young, T. S.; Ahmad, I.; Yin, J. A.; Schultz, P. G. *J. Mol. Biol.* 2010, *395*, 361-374.
(4) Hong, S. H.; Kwon, Y.C.; Martin, Y.W.; Des Soye, B.J.; de Paz, A.M.; Swonger, K.N.; Ntai, I.; Kelleher N.L.; Jewett, M.C. *Chem. Bio. Chem.* 2015, *16*, 844-853
(5) Di Biasio, A.; Bolle, G.; Cametti, C.; Codastefano, P.; Tartaglia, P. In *Trends in Colloid and Interface Science V*; Corti, M., Mallamace, F., Eds.; Steinkopff: 1991; Vol. 84, p 359-361.
(6) Patterson, J. P.; Sanchez, A. M.; Petzetakis, N.; Smart, T. P.; Epps III, T. H.; Portman, I.; Wilson, N. R.; O'Reilly, R. K. *Soft Matter* 2012, *8*, 3322-3328.
(7) Kline, S. *J. Appl. Crystallogr*. 2006, *39*, 895-900.
(8) Konarev, P. V.; Volkov, V. V.; Sokolova, A. V.; Koch, M. H. J.; Svergun, D. I. *J. Appl. Crystallogr*. 2003, *36*, 1277-1282.
(9) Guinier, A.; Fournet, G. *Small-angle scattering of X-rays*; John Wiley & Sons: New York, 1955.
(10) Glatter, O.; Kratky, O. *Small-Angle X-Ray Scattering*; Academic Press, 1982.